Acta Geochim (2023) 42(2):266–289
https://doi.org/10.1007/s11631-022-00577-4

ORIGINAL ARTICLE

Identification of major sources controlling groundwater geochemistry in Mount Makabaï in the Far-North of Cameroon (the northernmost part of the Pan-African Belt)

Merlin Gountié Dedzo[1] · **Désiré Tsozué**[2] · **Amidou Kpoumié**[2] · **Aubin Nzeugang Nzeukou**[2]

Received: 23 December 2021 / Revised: 30 September 2022 / Accepted: 10 October 2022 / Published online: 10 November 2022

Abstract The present work focuses on the volcanic basement rock geochemistry of Mount Makabaï (Maroua-Cameroon city) in relation to groundwater geochemistry. Investigations were centered on an approach involving an association of several methods such as geological cartography, hydrogeology, and geochemistry. Three rock samples, four disturbed soil samples, three undisturbed soil samples, and 20 samples of groundwater in 10 wells were collected during fieldwork and prepared for laboratory analyses. Bedrocks exhibit porphyritic, aphyric, and subaphiric textures. The phenocryst phases are mainly olivine, clinopyroxene, and plagioclase. Based on whole rock major element chemical compositions, the Makabaï samples, plotted on $Na_2O + K_2O$ versus SiO_2 diagram, are mugearite, hawaiite, and basalt. The ratio of $(MgO + CaO)/(Na_2O + K_2O)$ exceeds unity and shows dominance of alkaline Earth metals (MgO: 2.99–4.48 %; CaO: 6.19–9.80 %) relatively to alkali metals (Na_2O: 2.27–4.46 %; K_2O: 2.09–2.51 %). Exchangeable base contents are high, mostly represented by Ca and Mg, whose contents vary from 14.6 to 35.28 cmol(+) kg^{-1} and from 3.28 to 9.48 cmol(+) kg^{-1} respectively. The CEC_{clay} is likewise high, fluctuating between 116.80 and 181.38 cmol(+) kg^{-1}, values in line with the presence of 2:1 clay minerals represented in the study area by montmorillonite. In the water samples, the Ca^{2+} and Na^+ contents are generally higher than K^+ and Mg^{2+}, reflecting the relative abundance of Na_2O and CaO oxides to K_2O and MgO oxides in rocks where different waters were sampled. The waters of Makabaï are acidic to neutral ($6.3 \leq pH \leq 7.4$) and weakly to highly mineralized ($110.0 \leq EC \leq 1190.0$ µS/cm). Hydro-geochemical classification by using the Piper diagram revealed two water types: (1) $CaMg–HCO_3$ (40%) and (2) CaMg–Cl or $CaMg–SO_4$ (60%). The average content of ions in all the analyzed samples was $HCO_3^- \gg NO_3^- > SO_4^{2-} > Cl^-$ for anions and $Ca^{2+} \gg Mg^{2+} > Na^+ > K^+$ for cations. Major mechanisms governing ionic constituents of groundwater in the study area are water–rock interactions, silicate weathering, and ion exchange.

Keywords Mount Makabaï-Maroua city · Far-North Cameroon · Bedrock minerals · Groundwater-rock-soil interaction · Crystalline basement

1 Introduction

Water plays a fundamental role for living things, particularly in socio-economic development and ecosystems (Selvam et al. 2013; An et al. 2014; Ma et al. 2014; Eshtawi et al. 2016). Water security is a challenge for the developing world today. Thus, numerous studies carried

---

✉ Désiré Tsozué
tsozudsir@yahoo.fr

Merlin Gountié Dedzo
merlin.gountie@gmail.com; merlinodedzo@yahoo.fr

Amidou Kpoumié
amidou27@yahoo.fr

Aubin Nzeugang Nzeukou
nzeuk@yahoo.fr

[1] Department of Life and Earth Sciences, Higher Teachers' Training College, University of Maroua, P.O. Box. 55, Maroua, Cameroon

[2] Department of Earth Sciences, Faculty of Science, University of Maroua, P.O. Box. 814, Maroua, Cameroon

out across the world allow assessing the physicochemical and bacteriological quality of water resources and this is related to the problems of which the populations are victims in their different concerned areas. The quantity and quality of these water sources are influenced by geographic location and environmental factors, such as the chemical nature of the underlying rocks, precipitation inputs, and soils formation (Van der Merwe 1962; Djeuda 1987; Furry 1997; Derron 1999; Faniran et al. 2001; Adeli et al. 2021), but also on the vegetation and human activities. The chemical nature of rainwater that infiltrates through the vadose zone to reach the saturated zone is altered by geochemical reactions with regolith minerals which increase the contents of groundwater major elements (Siva and Kamble 2017). The quality of groundwater is evaluated by its physicochemical and biological characteristics which may be affected by population density, urbanization, industrialization, pressure on the resource, and lack of a reliable sanitation network (Martin del Campo et al. 2014; Khazaei et al. 2004; Brindha and Kavitha 2015). Because of this, water–rock interaction has been defined as the sum of exchanges that happen between rocks and waters that are in contact with them (Zuddas 2010). Soil structure and quality also play a major role in the evolution of groundwater chemistry. Soil physical properties and chemistry of groundwater plays also a vital role in the characterization of the suitability of the latter for irrigation (Patel et al. 2019). The importance of the relationships between minerals of aquifer and water in the origin/genesis and quality of groundwater was also underlined (Srinivasamoorthy et al. 2013).

In the Far-North and North regions of Cameroon, groundwater remains the main source of water consumption (Djaouda et al. 2014; Bello et al. 2019). It also allows populations to practice irrigation in unfavorable periods which lasts 7 to 8 months. Thus, it also plays a significant role in the socio-economic development of the region. The latest population census in Cameroon showed that the Far-North region has the highest population density in the country (BUCREP 2011) and only 13.8 % of families had access to drinking water in 2011 (Djao et al. 2011). Although these groundwaters are the most used for their supposedly good quality at least on a purely physical level (clear and transparent waters), they have very little or almost unknown physicochemical and bacteriological characteristics. Some studies evaluating the quality of the water in the northern zone of Cameroon report many sources of pollution (Mbawala et al. 2010; Djaouda et al. 2014; Kristin et al. 2014; Hambaté et al. 2015; Sara et al. 2016), which is a threat because it lowers the overall water resources balance. Other studies already carried out also in this region have focused much more on the hydrochemical and isotopic aspects (Ketchemen 1992; Ngounou Ngatcha 1993; Fantong et al. 2009; Bello et al. 2019), than the connection with the groundwater recharge phenomenon (Ketchemen 1992; Ngounou Ngatcha 1993), and recharge modeling (Leblanc et al. 2007; Boronina et al. 2008; Candela et al. 2014; Cheo et al. 2017). All these studies at the local scale did not consider the analysis of lithological aspects and understanding of water quality. From these studies, we note concentrations of some chemicals (Ketchemen 1992; Fantong et al. 2009; Ketchemen et al. 2016; Bello et al. 2019) and bacteriological elements (Djaouda et al. 2014) sometimes beyond the standards recommended by the WHO in an environment where industries are rare. Studies in this region also show that fluorite concentrations are very high and sometimes above the WHO recommended standard (Fantong et al. 2009, 2010, 2019). Studies that have taken into account the influence of lithological aspects on the water quality are carried out more now in several regions of Cameroon and also in other parts of Africa (Gountié Dedzo et al. 2017; Kurdehlachin et al. 2018; Adabanija et al. 2019). Groundwater quality evaluation is a complex procedure that undertakes many variables which can cause various stresses on the quality of water (Bodrud-Doza et al. 2016). Thus, such studies have been introduced on areas where the geological formations are mainly covered with gneiss, granite, and amphibolite (Gountié Dedzo et al. 2017), rhyolite (Kurdehlachin et al. 2018), granite, piedmont alluvium, and Basalt (Fantong et al. 2019), gneiss, migmatite, stromatolite, quartzite, and a granitic component of the migmatite gneiss (Adabanija et al. 2019). The populations of the regions of the North and the Far North sometimes complain about the water quality of certain productive boreholes and wells. These waters sometimes have very pronounced tastes, very high hardness, salinity, and scaling phenomena. Therefore, these boreholes and wells although cost enormous financial means, are sometimes abandoned. On the field and sometimes in the same area, from one well to another, the water quality can sometimes deteriorate or improve. To try to understand these phenomena and provide explanations, it would be interesting to conduct a study that links the water quality of the region and its lithology, since most studies that have previously been done in the region were limited to rock, or soil formations or on waters only. No study has yet attempted tried to combine these three aspects to understand water quality in the Northern zone of Cameroon and the origins of the chemical species present. Also from these studies, volcanic rocks are not sufficiently represented, and they did not combine rock and soil analyses to better substantiate the origins of the various minerals in the waters. However, although principles of water chemistry in rocks of volcanic nature are similar to those in other formations (Langmuir 1997; Mazor 2004; Appelo and Postma

2004), the weathering of these volcanic rocks in the Sudano-Sahelian region remains a curiosity. This study looks at understanding the chemistry of bedrocks in the crystalline basement of Mount Makabaï (Maroua-Cameroon city) and its weathering products in relation to groundwater chemical composition.

2 Materials and methods

2.1 Study area

Situated between the 14°13′ and 14°21′ eastern meridians and the 10°31′ and 10°38′ northern parallels, the study zone is located in Maroua city (Cameroon) (Fig. 1). The climate is a Sudano-Sahelian type, characterized by two seasons consisting of 8 months of the dry season (October–May) and 4 months of the rainy season (June–September) (L'hote 2000). The mean yearly pluviometry is 757.2 mm. Temperature ranges between 28 and 45 °C and the mean yearly air temperature is about 28.53 °C (Fig. 2). The study zone is a rounded dissymmetric hill-oriented SW-NE, with altitudes ranging between 395 and 722 m. Soils are mainly poorly or minimally developed soils. Maroua belongs to the Tsanaga hydrographic basin globally extends between 10°30′ N and 10°53′ N and between 13°42′ E and 14°36′ E. The hydrographic network is characterized by small seasonal collectors like Mayo Mizao and Mayo Kaliao, which drain the waters to Mayo Tsanaga which is the main river of Maroua town (Fig. 3).

2.2 Geological setting

The Makabaï study zone is an extension of the Poli Belt which belongs to the northernmost portion of the Pan-African Belt of Cameroon. The northern portion of Cameroon (Fig. 1) is characterized by variability of geological formations:

- Neoproterozoic high, medium- to low-grade gneisses and schists of the Poli Belt which have a sedimentary, volcano-sedimentary, and volcanic origin (Toteu 1990; Ngako 1999; Penaye et al. 2006; Toteu et al. 2006; Bouyo Houketchang et al. 2009; Bouyo et al. 2015).

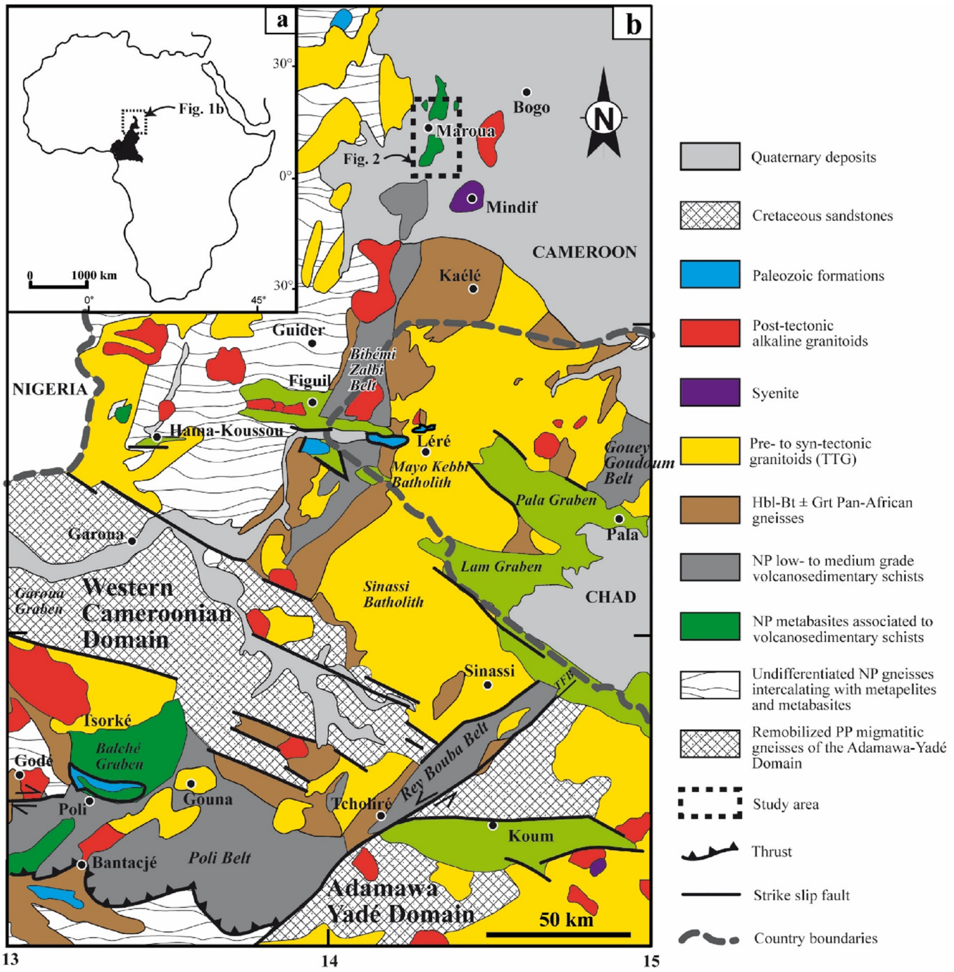

Fig. 1 Location of the study site: **a** location of Cameroon in Africa; **b** geological map of Northern Cameroon and Southwestern Chad (modified from Bouyo et al. 2015). TBF: Tcholliré-Banyo Fault; NP: Neoproterozoic; PP: Paleoproterozoic

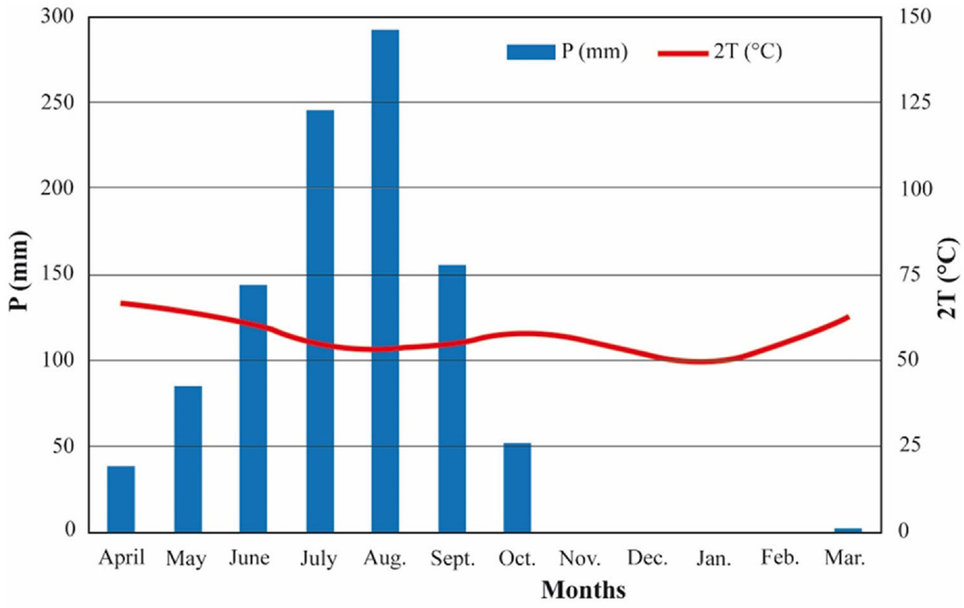

Fig. 2 Ombrothermal diagram at the Maroua-Salak station (representative the semi-arid climate of the Far-North Region Cameroon), 1980–2011

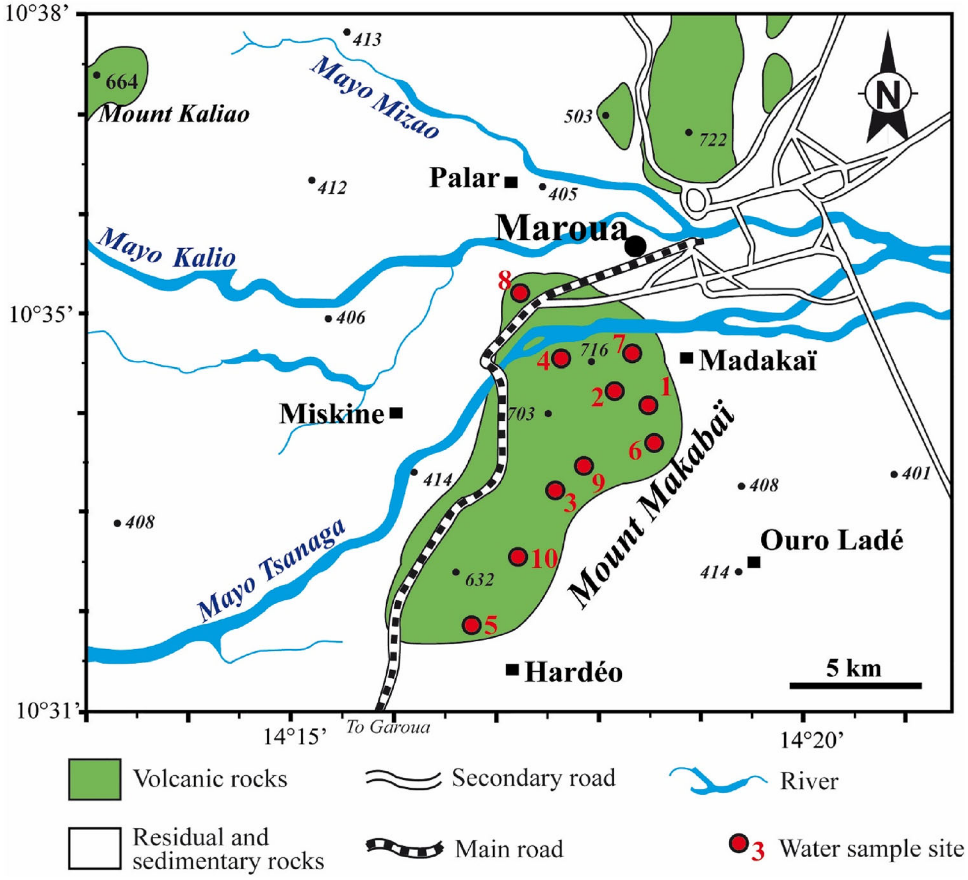

Fig. 3 Geological map of the study area and the water sampling sites

The Poli Belt characterizes a syn- to a pre-collisional basin that was made in the context of a magmatic arc or established upon, or in the environs of recent magmatic arcs. The filling of this basin happened in a back-arc/docking-arc context (Toteu et al. 2006). Metavolcanics are calcalkaline rhyolite and tholeiitic basalt emplaced in an extensional crustal environment (Njel 1986; Toteu 1990; Ngako 1999; Penaye et al. 2006; Toteu et al. 2006; Bouyo Houketchang et al. 2009; Bouyo et al. 2015). The depositional period is estimated between 700 and 665 Ma; detrital sources include ca. 736, 780, 830, and 920 Ma magmatic rocks (Toteu et al. 1987, 2006);

- Pan-African pre-, syn- and late-tectonic calc-alkaline granitoids emplaced between 660 and 580 Ma (Toteu et al. 2001; Penaye et al. 2006);
- Post-tectonic alkaline granitoids including felsic and mafic dykes cross-cut by intrusive syenites and granites; followed by the setting up of numerous basins made of unmetamorphosed volcanic rocks and sediments (Toteu et al. 2004; Van Schmus et al. 2008).

The geological sketch map of the Makabaï study area (Fig. 3) realized after field studies, is composed of volcanic rocks and recent quaternary deposits (residual and sedimentary rocks).

2.3 Sampling and analytical procedure

2.3.1 *Sample collection*

This phase begins with soil description from representative soil profiles dug down to about 2 m in the weathering horizon. Soil samples were collected in each horizon of the soil profiles from the bottom upwards, after they have been cleaned from the top downwards, according to Baize and Jabiol (1995). A sampling operation, preceded by the cartography of water points, was done in December 2016, to understand the water quality of the samples from the wells. Six rock samples, four disturbed (for physicochemical analyses) and three undisturbed (for microscopic analyses) soil samples, and 20 samples of water in 10 wells (2 samples per well) were collected during fieldwork and were prepared for laboratory analyses. The water samples were collected during two different campaigns carried out on the same hydraulic structures (wells) respectively in December 2017 and in December 2018 that is 2 × 10 structures.

2.3.2 *Analytical procedures*

Chemical and petrographic analyses were carried out on rock and soil samples. To characterize the mineralogy and textures of the Makabaï rock samples and their weathering products, optical studies using a polarizing microscope were realized on thin sections from representative samples. Soil thin sections were obtained after impregnation with resin and then hardening in the air following the protocol of Hanrion (1976). Soil thin sections were described following the guideline of Stoops (2003). Chemical analysis of 3 rock samples was performed in the framework of this study. 5 g of homogenous powder was used for analyses. Whole-rock, soil, and water analyses were done following the procedures described by Gountié et al. (2017). Soil analyses have allowed us to understand the composition of the soil solution. The parameters determined include clay content, pH, organic carbon, exchangeable cations (Ca^{2+}, Mg^{2+}, K^+, Na^+), cation exchange capacity (CEC), total nitrogen, and available phosphorus and chlorine. The clay fraction was determined by the pipette method. Soil pH was measured potentiometrically in a 1:2.5 soil:solution ratio. Chloride ion was determined by potentiometric titration. The quantity of total nitrogen was evaluated by titration after the mineralization of organic matter and distillation. Exchangeable cations are shifted by ammonium acetate (CH_3COONH_4) at pH 7. The proportions of K^+ and Na^+ were evaluated by flame photometry. Those of Ca^{2+} and Mg^{2+} were determined by complexometry. Organic carbon was determined by the Walkley and Black method. Soil organic matter (OM) content was obtained by multiplying soil organic carbon (OC) content by 1.724. Available phosphorus was determined by the Bray-2 method. Concerning the water analysis, the multi-parameter EXTIC II brand was used for the determination of the conductivity, TDS, alkalinity, and pH. The pH values were read on the multi-parameter after prior calibration of the pH meter using the buffer of 7, 4, and 10 values. Chemical concentrations, including cations (Ca^{2+}, Mg^{2+}, Na^+, K^+, ${NH_4}^+$) and anions (${SO_4}^{2-}$, Cl^-, ${NO_3}^-$, ${PO_4}^{3-}$, F^-) were determined by colorimetric assay using a UV-VISRS/2500 spectrophotometer. The wavelengths used for the determination of these concentrations differ from one ion to another. ${HCO_3}^-$ ion was determined by titration. The charge balance error percentage (%CBE) was also calculated for each sample using the following Eq. (1):

$$\%CBE = \frac{TZ^+ - TZ^-}{TZ^+ + TZ^-} \times 100 \qquad (1)$$

where TZ^+ indicates the total concentrations of cations and TZ^- indicates the total concentrations of anions. Both cations and anions are expressed in milliequivalent per liter (meq/L).

The 20 water samples analyzed have a charge balance error percentage of less than 5 % as suggested by Domenico and Schwartz (1998), hence the use of these data. This result is consistent with other previously published analyses in the same area (Bello et al. 2019) but also in other areas of the world (Li et al. 2018).

3 Results

3.1 Petrographic and geochemical characterization of geologic formations

Volcanic rocks of the studied area are outcropped as bowls on the flanks of Makabaï Mountain and are characterized in some places by columnar joints delimiting prisms in the summit of the massif. Rock samples exhibit porphyritic, aphyric, and sub-aphiric textures (Fig. 4a–f). The phenocryst phase is mainly olivine, clinopyroxene, and plagioclase (Fig. 4b, d, f). Calcite is identifiable in some cracks in the rock (Fig. 4c, d). Olivine, often altered to red-brown iddingsite, occurs in some samples. The groundmass consists of dominant microlites of plagioclases alongside clinopyroxene, olivine, and oxides.

Based on whole rock major element chemical compositions (Table 1), the Makabaï samples, plotted on $Na_2O + K_2O$ versus SiO_2 diagram (Le Bas et al. 1986) (Fig. 5), are mugearite, hawaiite, and basalt. According to the subalkaline–alkaline limit of Irvine and Baragar (Irvine and Baragar 1971), the basaltic formations are all alkaline. The ratio $(MgO + CaO)/(Na_2O + K_2O)$ is, respectively, 1.40, 2.80 and 2.82. This parameter exceeds unity and shows dominance of alkaline Earth metals (MgO: 2.99–4.48 %; CaO: 6.19–9.80 %) relatively to alkali metals (Na_2O: 2.27–4.46 %; K_2O: 2.09–2.51 %). The abundance of plagioclase, pyroxene, olivine, and calcite reflects the high contents of alkaline Earth metals in these rocks. In the water samples, the content of Ca^{2+} and Na^+ are generally higher than K^+ and Mg^{2+}, reflecting the relative abundance of the oxides Na_2O and CaO to the K_2O and MgO oxides in rocks where different waters were sampled.

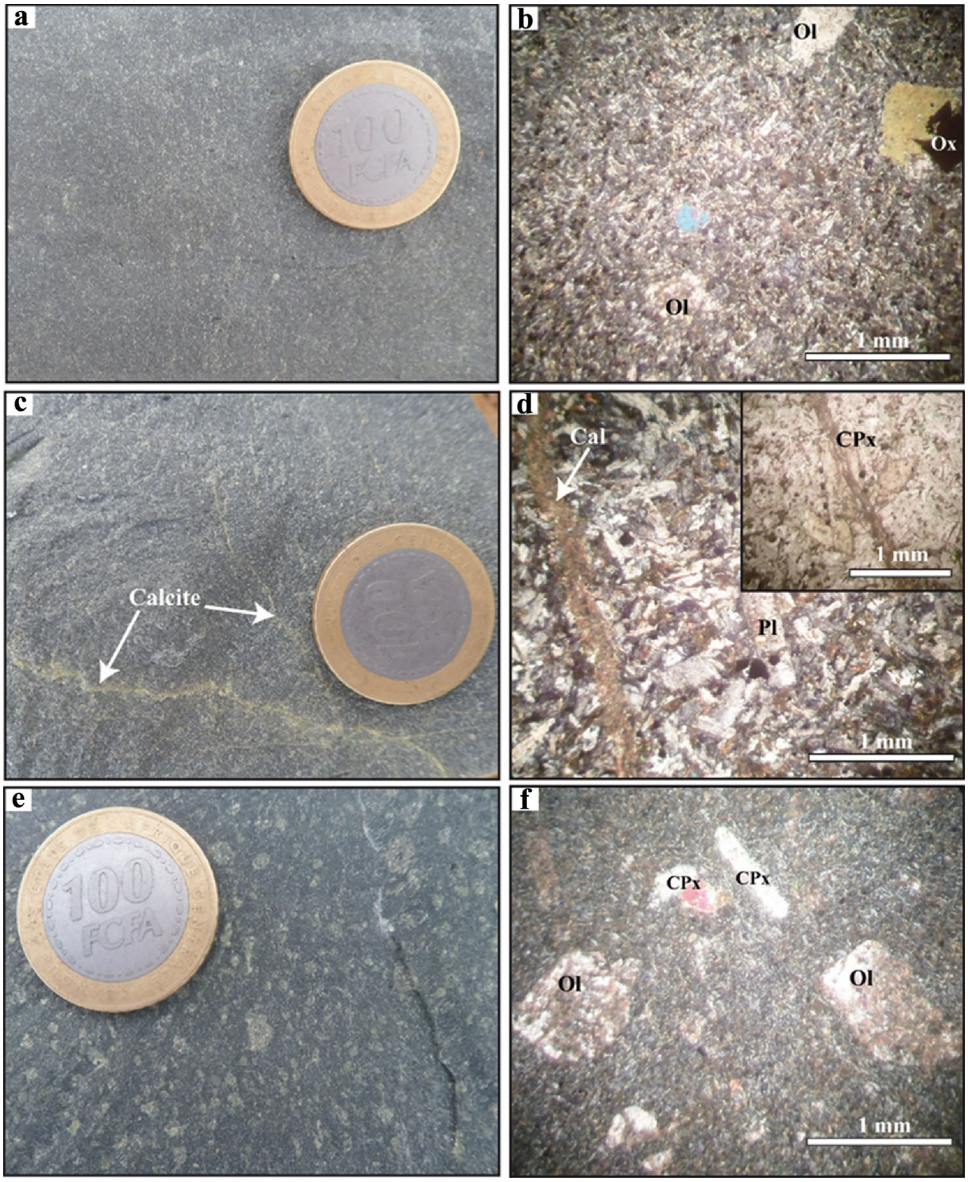

Fig. 4 **a** Sample of mugearite with aphyric texture and **b** the corresponding microphotograph. **c** Sample of hawaiite with sub-aphyric texture and **d** the corresponding microphotograph showing secondary crystallization of calcite; inset: microphotograph of this basalt in natural light with association of clinopyroxenes. **e** Sample of basanite with porphyritic texture and **f** the corresponding microphotograph. Ol: olivine. CPx: clinopyroxene. Pl: plagioclase. Cal: calcite

Table 1 Major elements data for the studied area rocks

Rocks	Samples	SiO_2	TiO_2	Al_2O_3	Fe_2O_3	MnO	MgO	CaO	Na_2O	K_2O	P_2O_5	Cr_2O_3	LOI	Total	$Na_2O + K_2O$	MgO + CaO	$(MgO + CaO)/(Na_2O + K_2O)$
Hawaiite	MK1	48.24	0.85	18.65	9.74	0.15	4.48	9.80	2.98	2.09	0.34	0.006	2.4	99.73	5.07	14.28	2.82
Basalt	MK2	49.46	0.87	19.43	8.55	0.16	3.89	9.49	2.27	2.51	0.40	0.005	2.7	99.74	4.78	13.38	2.80
Mugearite	MK3	54.92	0.96	17.36	8.43	0.16	2.99	6.19	4.46	2.09	0.59	0.003	1.5	99.65	6.55	9.18	1.40
	Mean	50.873	0.893	18.48	8.906	0.156	3.786	8.493	3.236	2.23	0.443	0.005	2.2	99.705	5.467	12.28	2.34

3.2 Morphological characteristics of weathering material

Field descriptions permit to note that the studied weathered materials are composed of four main horizons, from bottom to top, as follows (Fig. 6):

200–75 cm: a yellowish C horizon (10YR 7/8). It is compact, and massive, with many fissures; under the microscope, there are no primary minerals and many remnants of altered plagioclases shape are observed;

75–30 cm: a reddish yellow BC horizon (7.5YR 6/8). The texture is loamy. The structure is massive. Fissures are still present, and compact blocks observed below are embedded here in the loose matrix; remnants of altered primary mineral shapes had almost disappeared;

30–7 cm: a reddish yellow loose B horizon (5YR 6/8). The texture is loamy clayey. The structure is weakly blocky to massive. The horizon is characterized by high matrix porosity. Many rootlets are present; remnants of altered primary mineral shapes are not visible. The groundmass had a vughy microstructure and reddish micromass.

7–0 cm: a humiferous yellowish red A horizon (5YR 5/8). It is characterized by a loamy clayey texture and a weakly expressed lumpy structure. The horizon is characterized by high matrix porosity. There are many rootlets.

Percolated water passed through the soil section before reaching the water table, which in this landscape is in the saprolite. The development of the saprolite porous network depends on the grain size of the minerals being dissolved. This dissolution of crystal grains increases porosity, favoring the circulation of water and the leaching of elements. The quality of water will therefore reflect the composition of the soil solution.

3.3 Physicochemical characteristics of soil solutions

Table 2 presents the physicochemical results of soil samples. Soil pH values vary slightly along the profile (CV < 15 %). They ranged from slightly acidic (5.90) in the humiferous horizon to slightly above neutral (7.50) in the fine saprolite. pH_{KCl} values are below those of pH_{Water} in all horizons. Clay contents are constant along the soil profile (CV = 1.90 %), ranging between 45.00 and 47.00. Organic carbon (OC) contents are low to very low, ranging from 0.36 in the lower horizon to 0.65–0.73 % in the superior portion of the profile. Similarly, nitrogen contents are low to very low. Exchangeable base contents are high, mostly represented by Mg and Ca whose contents vary from 14.6 to 35.28 cmol(+) kg^{-1} and from 3.28 to 9.48 cmol(+) kg^{-1} corresponds to mean values of 24.42 ± 8.70 and 6.22 ± 2.84 cmol(+) kg^{-1} respectively. The CEC is high, fluctuating between 53.7 and

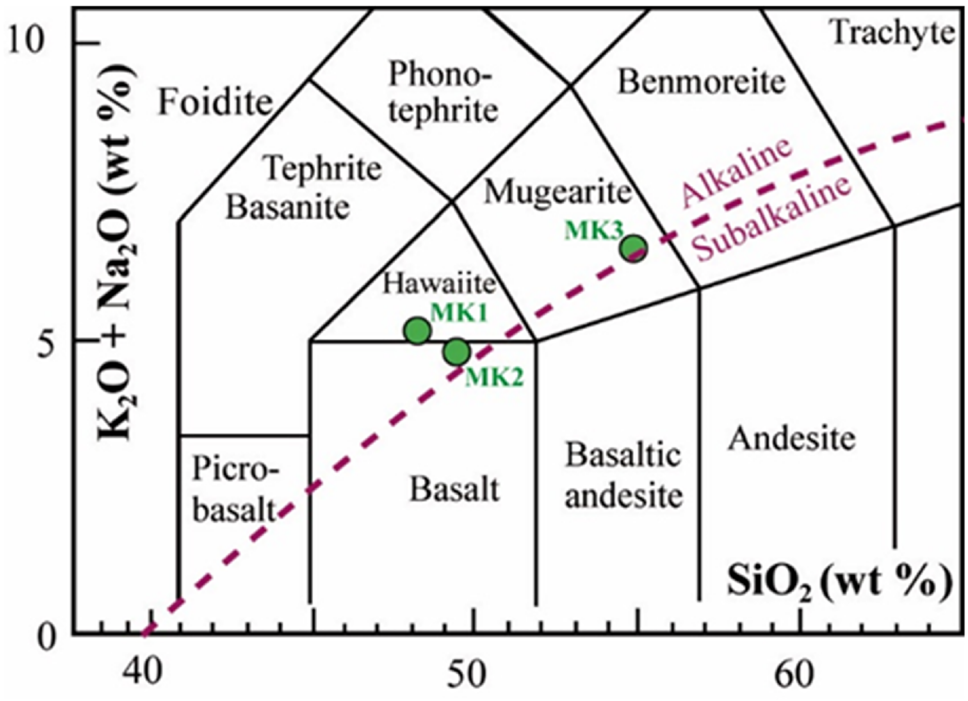

Fig. 5 Total alkali versus silica classification diagram (after Le Bas et al. 1986). The alkaline-subalkaline dividing line is from Irvine and Baragar (1971)

82.9 cmol(+) kg^{-1}, corresponding to a mean value of 67.70 ± 13.03 cmol(+) kg^{-1}. The CEC_{clay} is moreover high, ranging between 116.8 and 181.4 cmol(+) kg^{-1} (Table 2), values in line with the presence of 2:1 clay minerals represented in the Makabaï study area by montmorillonite already identified by (Tsozué and Ndjigui 2017). Available phosphorus concentrations are low in the humiferous surface horizon (8.77 mg/kg), but increase with depth, reaching 61.01 mg/kg in the horizon C at the lowest zone of the profile. Globally, no significant correlation was noted between soil parameters at $p < 0.05$. However, at $p < 0.1$, little significant correlation was noted between Ca^{2+} and pH_{Water}, Mg^{2+} and Cl^-, P_2O_5 and Cl^-, P_2O_5 and Mg^{2+}, Na^+ and K^+, Na^+ and CEC, Na^+ and CEC_{clay} (Table 3).

3.4 Physicochemical characteristics of water samples

Table 4 presents physicochemical data of the Makabaï groundwater. The pH values are neutral for all samples and vary slightly (CV < 15%) along the studied area between 7.14 and 8.10 (mean: 7.59 ± 0.29; $n = 20$). The values TDS (560–2313 mg/L) and EC (591–2440 µS/cm) vary considerably (CV > 35%), with an average of 1040.05 mg/L and 1085.25 µS/cm respectively. The alkalinity of samples also varies substantially (CV > 35%); their values oscillate between 480 and 8509 mg/L (mean: 3253.15 mg/L; Table 4). It is necessary to remark that the maximum pH, EC, TDS, and TH values were found in well W2, whereas the maximum value of alkalinity was measured in well W10. The lowest value of EC, pH, and TDS are measured in well W7, while well W9 present the lowest TH value.

K^+ and Na^+ are present respectively in proportions of 1.31 and 62.04 mg/L (mean: 11.65 ± 17.50 mg/L) and 14.67 and 140.58 mg/L (mean: 57.64 ± 39.57 mg/L; Table 4). On the other hand, the contents of Mg and Ca respectively oscillate between 54.51 and 198.41 mg/L (mean: 112.37 mg/L) and between 13.99 and 67.64 mg/L (mean: 38.53 mg/L). NH_4^+ contents fluctuate from 0 to 1.73 mg/L (mean: 0.71 mg/L). Generally, the contents of cations are considerably variable, with a CV > 35 %. Only the contents of K^+ are highly variable (CV > 100 %). The highest contents were found in the wells W1 (Na^+), W2 (K^+, Ca^{2+}, and Mg^{2+}), and W8 (NH_4^+) whereas the minimum values are measured in the wells W4 (NH_4^+), W6 (Na^+, NH_4^+), W7 (K^+, NH_4^+) and W9 (Mg^{2+}, Ca^{2+}) (Table 4).

NO_3^- and Cl^- concentrations are respectively between 3.62 and 271.83 mg/L (mean: 103.31 mg/L) and between 5.76 and 39.68 mg/L (mean: 17.91 mg/L). The HCO_3^- and F^- contents vary respectively from 29.28 to 519 mg/L (mean: 198.42 mg/L) and from 0.5 to 1.53 mg/L (mean: 0.88 mg/L). The contents of these anions are considerably variable (CV > 35 %). For these four ions, the maximum values were measured in wells W1 (NO_3^-), W2 (Cl^-), W3 (F^-), and W10 (HCO_3^-) whereas the lowest content is

Fig. 6 Macroscopic organization of the studied soil profile

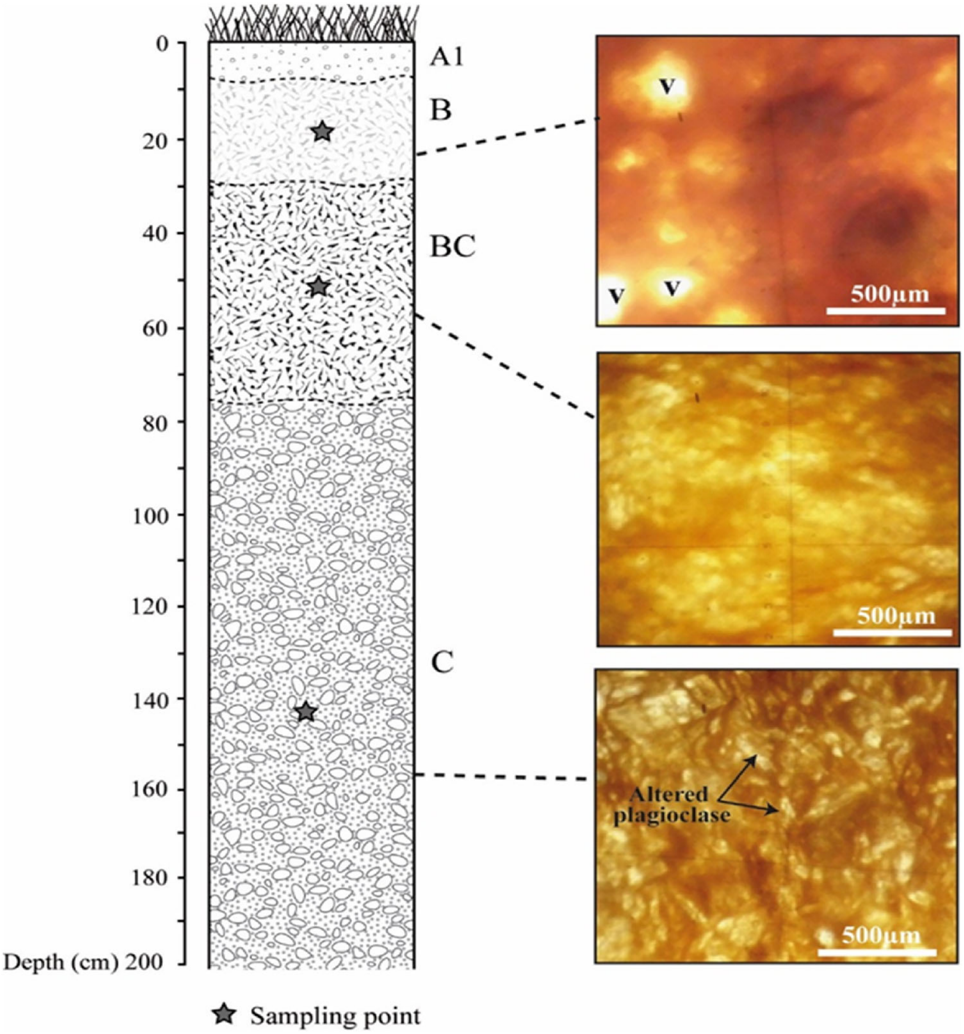

Table 2 Physicochemical results of soil samples

Horizons	pH_{water}	pH_{KCl}	Cl^- (mg/l)	Clay (%)	OC (%)	OM (%)	N (%)	Ca Cmol(+)	Mg kg^{-1}	K	Na	CEC	CEC_{clay}	P_2O_5 (mg/kg)
A1	5.90	5.20	4.25	45.00	0.65	1.13	0.11	14.56	3.28	0.78	0.65	53.68	116.80	8.77
B	6.20	4.80	22.69	45.00	0.73	1.25	0.09	21.52	4.48	0.42	1.09	82.88	181.38	10.31
BC	7.50	6.00	34.04	47.00	0.55	0.94	0.10	35.28	7.64	0.42	0.87	73.52	154.41	33.02
C	6.80	5.00	45.38	45.00	0.36	0.63	0.07	26.32	9.48	0.42	0.87	60.72	133.55	61.01
Min	5.90	4.80	4.25	45.00	0.36	0.63	0.07	14.56	3.28	0.42	0.65	53.68	116.80	8.77
Max	7.50	6.00	45.38	47.00	0.73	1.25	0.11	35.28	9.48	0.78	1.09	82.88	181.38	61.01
Mean	6.60	5.25	26.59	45.50	0.573	0.988	0.093	24.420	6.220	0.510	0.870	67.700	146.535	28.278
SD	0.707	0.526	17.53	1.00	0.16	0.27	0.017	8.70	2.847	0.180	0.180	13.033	27.863	24.476
CV (%)	9.30	8.70	57.10	1.90	24.20	23.70	16.00	30.90	39.60	30.60	17.90	16.70	16.50	75.00

measured in wells W3 (Cl^-), W6 (HCO_3^-) W9 (F^-, NO_3^-). The SO_4^{2-} concentrations vary from 7.63 to 188.81 mg/L (mean: 38.01 mg/L); their contents are greatly variable (CV > 100 %). The highest content is found in well W2, while the minimum is identified in well W7.

Table 3 Spearman's correlation coefficients for physicochemical parameters of soil samples

Variables	pH_{water}	pH_{KCl}	Cl-	OC	OM	N	Ca	Mg	K	Na	CEC	CEC_{clay}	P_2O_5
pH_{water}	**1**												
pH_{KCl}	0.400	**1**											
Cl-	0.800	0.000	**1**										
OC	− 0.600	− 0.400	− 0.800	**1**									
OM	− 0.600	− 0.400	− 0.800	1.000	**1**								
N	− 0.400	0.600	− 0.800	0.400	0.400	**1**							
Ca	1.000	0.400	0.800	− 0.600	− 0.600	− 0.400	**1**						
Mg	0.800	0.000	1.000	− 0.800	− 0.800	− 0.800	0.800	**1**					
K	− 0.775	0.258	− 0.775	0.258	0.258	0.775	− 0.775	− 0.775	**1**				
Na	0.316	− 0.632	0.316	0.316	0.316	− 0.632	0.316	0.316	− 0.816	**1**			
CEC	0.400	− 0.400	0.200	0.400	0.400	− 0.400	0.400	0.200	− 0.775	0.949	**1**		
CEC_{clay}	0.400	− 0.400	0.200	0.400	0.400	− 0.400	0.400	0.200	− 0.775	0.949	1.000	**1**	
P_2O_5	0.800	0.000	1.000	− 0.800	− 0.800	− 0.800	0.800	1.000	− 0.775	0.316	0.200	0.200	**1**

*Significant at $p < 0.05$

4 Discussion

4.1 Physical properties

Table 4 presents the physiochemical parameters for all 20 samples of water. The pH values of these samples are below the WHO guideline and indicate that the waters were commonly neutral. EC and TDS exhibited an important range of values with high standard deviations (506.5 and 538.42 respectively), signifying the variability of the geochemical activities within the Maroua area groundwater (Kamtchueng et al. 2014, 2016). Concerning the quality of water for drinking, half of the investigated samples were fresh (TDS < 1000 mg/L), and another half were brackish (TDS > 1000 mg/L) (Kumar et al. 2007). With the same idea, the TH values indicate that 35% of the sampled waters were hard (193.63–294.14 mg/L) and very hard (304.12–773.35 mg/L) for the rest of the samples (Sawyer and McCartly 1967). TDS, EC, and TH parameters for wells W8, W5, W4, and W2 are generally near and above the WHO standard. The alkalinities of sampled water are all above the WHO guideline value. The buffering capacity also known as the alkalinity generally consists of HCO_3^- and CO_3^{2-} contents and indicates the capacity for groundwater to neutralize the inputs of acidity (Takem et al. 2015); this is the reason why there is a significant positive correlation between alkalinity and HCO_3^- (r = 1).

4.2 Hydrogeochemical facies and classification

The geochemistry of waters is principally linked to the geology as well as the anthropogenic activities and geochemical processes which take place within the aquifer system. Piper diagram (Piper 1944) is frequently used to characterize and define water types. From trilinear plot presented in Fig. 7a, (CO_3^{2-} + HCO_3^-) dominates (SO_4^{2-} + Cl^-), and (Ca^{2+} + Mg^{2+}) exceeds (Na^+ + K^+). The major ions concentrations (meq/L) plotted on a pie chart (Fig. 7b) indicated that HCO_3^- and Ca^{2+} were the major ions in waters followed by Mg^{2+} and NO_3^-. Two kinds of water have been identified using a Piper diagram, based on their relative proportions and ionic concentrations, (Fig. 7a). The CaMg-HCO_3 water type represents 40% and CaMg-NO_3Cl or CaMg-NO_3SO_4 type represents 60%. The presence of the CaMg-HCO_3 water types demonstrate that the mineral dissolution is probably the silicate and secondary carbonate minerals with abundant recharge from freshwater (Ako Ako et al. 2012). The major representation of the second type suggests mixing freshwater with water from contaminated sources. The average concentration (expressed in meq/L) of dissolved ions in all the analyzed samples was $HCO_3^- \gg NO_3^- > SO_4^{2-} > Cl^-$ for the

Table 4 Results of physicochemical analysis of the groundwater samples of the study area

Sample ID	pH	EC (μS/cm)	TDS (mg/L)	AlK (μeq/L)	TH (mg/L)	Na^+ (mg/L)	NH_4^+ (mg/L)	K^+ (mg/L)	Mg^{2+} (mg/L)	Ca^{2+} (mg/L	F^- (mg/L)	Cl^- (mg/L)	NO_3^- (mg/Ll)	PO_4^{3-} (mg/L)	SO_4^{2-} (mg/L)	HCO_3^- (mg/L)	pCO_2 (atm)
W1-1	7.41	1255	1190	6654	402.39	130.05	0.04	3.03	28.46	114.28	0.83	24.88	252.78	0.00	50.34	405.89	–1.82
W1-2	7.8	1359	1288	3948	426.38	140.58	0.02	2.93	29.65	121.93	1.09	24.39	271.83	0.00	54.03	240.83	–2.44
Mean	7.61	1307.00	1239.00	5301.00	414.39	135.31	0.03	2.98	29.05	118.11	0.96	24.63	262.31	0.00	52.19	323.36	–2.13
W2-3	8.1	2420	2294	1154	718.52	114.77	1.49	56.68	62.60	184.74	0.71	36.63	14.55	0.00	54.14	70.39	–3.27
W2-4	8.09	2440	2313	7704	773.35	122.65	1.53	62.04	67.64	198.41	0.87	39.68	11.21	0.00	188.81	469.94	–2.45
Mean	8.10	2430.00	2303.50	4429.00	745.93	118.71	1.51	59.36	65.12	191.57	0.79	38.16	12.88	0.00	121.48	270.17	–2.86
W3-5	7.46	780	739	698	282.63	76.31	0.59	1.86	25.74	70.84	1.53	5.76	67.73	0.00	15.62	42.58	–2.84
W3-6	7.43	768	728	784	304.12	37.01	0.01	1.70	22.20	85.24	0.77	7.57	31.95	0.00	16.78	47.82	–2.75
Mean	7.45	774.00	733.50	741.00	293.38	56.66	0.30	1.78	23.97	78.04	1.15	6.66	49.84	0.00	16.20	45.20	–2.80
W4-7	8.05	1347	1277	673	729.78	41.76	0.01	15.39	65.52	184.46	0.73	25.66	183.65	0.00	37.88	41.05	–3.46
W4-8	8.01	1351	1281	741	717.98	41.38	0.00	16.15	64.19	181.91	0.85	25.26	201.58	0.00	33.02	45.20	–3.37
Mean	8.03	1349.00	1279.00	707.00	723.88	41.57	0.01	15.77	64.86	183.18	0.79	25.46	192.62	0.00	35.45	43.13	–3.42
W5-9	7.83	1134	1075	736	595.86	26.17	0.05	24.27	49.63	156.95	0.77	21.35	184.94	0.00	79.94	44.90	–3.20
W5-10	7.58	1125	1066	712	621.30	31.15	0.02	6.80	63.63	144.16	1.50	8.84	38.19	0.00	14.70	43.43	–2.96
Mean	7.71	1129.50	1070.50	724.00	608.58	28.66	0.04	15.53	56.63	150.55	1.13	15.09	111.56	0.00	47.32	44.16	–3.08
W6-11	7.46	709	672	480	376.82	14.67	1.46	14.13	31.62	98.86	0.53	12.91	113.25	0.00	18.60	29.28	–3.00
W6-12	7.6	715	678	800	379.76	45.17	0.00	2.17	27.70	106.48	0.70	13.90	120.52	0.00	19.64	48.80	–2.92
Mean	7.53	712.00	675.00	640.00	378.29	29.92	0.73	8.15	29.66	102.67	0.61	13.41	116.88	0.00	19.12	39.04	–2.96
W7-13	7.14	593	562	747	236.00	63.74	0.00	1.31	21.58	59.00	0.61	6.75	27.80	0.00	17.08	45.57	–2.48
W7-14	7.22	591	560	748	294.14	17.04	1.07	5.85	31.21	66.47	0.74	5.98	95.76	0.00	7.63	45.63	–2.56
Mean	7.18	592.00	561.00	747.50	265.07	40.39	0.53	3.58	26.40	62.73	0.68	6.37	61.78	0.00	12.36	45.60	–2.52
W8-15	7.42	1172	1105	5680	514.40	45.33	1.73	5.49	51.5	121.3	0.85	31.52	139.73	0	38.69	346	–1.90
W8-16	7.53	1163	1097	5470	508.32	41.28	1.65	5.49	50.98	119.72	0.86	31.56	138.02	0	39.66	334	–2.02
Mean	7.48	1167.50	1101.00	5575.00	11.36	43.31	1.69	5.49	51.24	120.51	0.86	31.54	138.88	0.00	39.18	340.00	–1.96
W9-17	7.46	596	562	5745	196.13	19.09	0.75	2.01	14.22	55.13	0.64	10.33	5.32	0	20.8	350	–1.92
W9-18	7.42	593	559	6845	193.63	19.35	0.89	1.63	13.99	54.51	0.5	9.86	3.62	0.31	19.24	418	–1.80
Mean	7.44	594.50	560.50	6295.00	194.88	19.22	0.82	1.82	14.11	54.82	0.57	10.10	4.47	0.16	20.02	384.00	–1.86
W10-19	7.38	776	732	8509	248.03	58.03	1.6	2.44	23.72	60.31	1.26	7.89	79.36	0	16.74	519	–1.68
W10-20	7.41	778	734	6235	258.51	67.28	1.24	1.73	24.82	62.7	1.34	7.56	84.37	0	16.89	380	–1.84
Mean	7.40	777.00	733.00	7372.00	253.27	62.66	1.42	2.09	24.27	61.51	1.30	7.73	81.87	0.00	16.82	449.50	–1.76
*Standard** *DL PL*	6.5–8.5 9.50	500 1400	500 1000	– 200	100 500	< 20 200	– 0.5	12 100	50 150	75 200	– 1.5	200 600	10 50	5 50	200 400	200 300	–
Statistical data																	
Min	7.14	591	560	480	193.63	14.67	0	1.31	13.99	54.51	0.50	5.76	3.62	0	7.63	29.28	–1.80

Table 4 continued

Sample ID	pH	EC (µS/cm)	TDS (mg/L)	AlK (µeq/L)	TH (mg/L)	Na^+ (mg/L)	NH_4^+ (mg/L)	K^+ (mg/L)	Mg^{2+} (mg/L)	Ca^{2+} (mg/L	F^- (mg/L)	Cl^- (mg/L)	NO_3^- (mg/Ll)	PO_4^{3-} (mg/L)	SO_4^{2-} (mg/L)	HCO_3^- (mg/L)	pCO_2 (atm)
Max	8.10	2440	2313	8509	773.35	140.58	1.73	62.04	67.64	198.41	1.53	39.68	271.83	0.31	188.81	519	−3.46
Mean	7.59	1083.25	1040.05	3253.15	438.90	57.64	0.71	11.65	38.53	112.37	0.88	17.91	103.31	0.02	38.01	198.42	−2.53
SD	0.29	538.42	506.50	2967.78	195.01	39.57	0.70	17.50	18.65	48.85	0.30	11.21	82.60	0.07	39.94	181.01	0,59
CV (%)	3.7	48.4	47.5	88.9	43.3	66.9	96.6	146.3	47.2	42.4	33.3	61	77.9	435.9	102.4	88.9	−23.3

*WHO Standard (2004); DL and PL stand for desired limit and max permissible limit respectively; EC: electrical conductivity; TDS: total dissolved solids; AlK: alkalinity; TH: total hardness (as $CaCO_3$ in mg/L) = 2.5(Ca^{2+}) + 4.1 (Mg^{2+}); Max: maximum; Min: minimum; SD: standard deviation; CV: coefficient of variation; pCO_2: CO_2 partial pressure

anions and $Ca^{2+} \gg Mg^{2+} > Na^+ > K^+$ for the cations. The high content of HCO_3^-, Ca^{2+}, and Mg^{2+} suggests that the chemical weathering process happens in the aquifer system. Natural processes like the incongruent dissolution of carbonates and/or silicates in the rocks that react with CO_2 gas coming from the mineralization of soil organic matter and microorganisms or root respiration could be a mechanism that releases HCO_3^- and Ca, Mg, Na, K cations and into the groundwater.

Probable sources of HCO_3^- comprise the occurrence of organic substance in the aquifer that is oxidized to produce CO_2, which stimulates the dissolution of the minerals (Srinivasamoorthy et al. 2014). These weatherings bring to the groundwater HCO_3^-, Mg^{2+}, and Ca^{2+} (Khashogji and Maghraby 2013; Ganyaglo et al. 2010; Saha et al. 2019). HCO_3^- may also be coming from the dissolution of silicate (Gastmans et al. 2010). The maximum concentration of Ca, Na, and Mg in waters are due to clay minerals (Garrels 1976), represented in the Makabaï area by montmorillonite, illite, and kaolinite (Tsozué and Ndjigui 2017; Nguetnkam et al. 2008, 2014).

4.3 Mechanisms controlling water chemistry and ionic relations among dissolved species

4.3.1 Geogenic process

In Table 4, logarithmic values of partial pressures of CO_2 (Log pCO_2) calculated from alkalinity and pH ranged from − 3.46 to − 1.68 atm (mean: − 2.53 atm). Comparative to the atmospheric air (with pCO_2 of − 3.5 atm), the higher values of pCO_2 suggest that the waters have gained CO_2 either from the respiration of soil microorganisms associated with the decomposition of organic substances or from root respiration. Similar remarks have been made in groundwater along CVL (Tanyileke 1994; Njitchoua and Ngounou-Ngatcha 1997; Fantong et al. 2009; Ako Ako et al. 2011, 2012; Kamtchueng et al. 2014, 2016; Wirmvem et al. 2013). According to these authors, in volcanic fields, the solute composition of groundwater is ascribed to the incongruent reactions and the hydrolysis of the rock-forming minerals. These remarks are confirmed by (Gibbs 1970) plots indicating that water–rock interaction is the main process regulating the geochemistry of waters around the Makabaï area (Fig. 8).

The secondary minerals which are in equilibrium or nearly in equilibrium with the analyzed water were identified by activity diagrams (Fig. 9) of Korjinski (1948). This diagram indicates that the main proportion of the waters belongs to the montmorillonite stability field, indicating that montmorillonite is the main stable secondary phase for the Mount Makabaï groundwater.

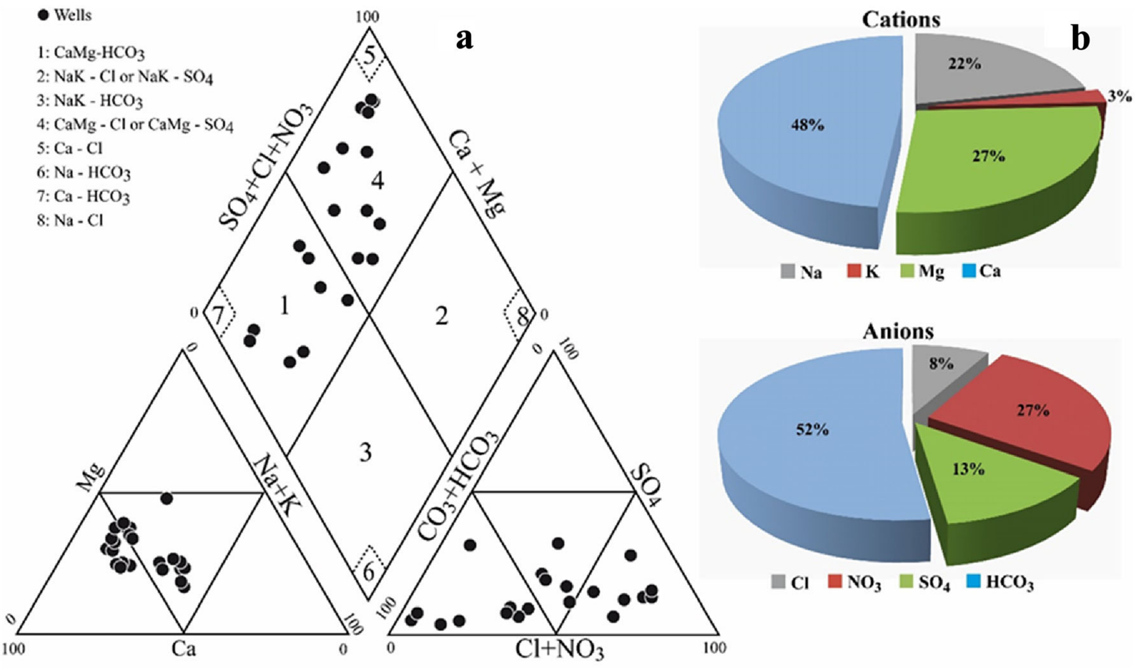

Fig. 7 **a** Piper (1944) diagram and **b** pie chart of mean concentrations of ions (meq/l) of water samples for the studied site presenting dominance of alkaline Earth metals (Ca + Mg) and weak acids (CO_3 + HCO_3) greatly exceed alkali metals (Na + K) strong acids (SO_4 + Cl) respectively

Fig. 8 Gibbs (1970) plots indicating water–rock interaction as main process regulating the chemistry of waters around Makabaï area. **a** TDS versus (Na + K)/(Na + Ca + K) diagram; **b** TDS versus Cl/(Cl + HCO_3)

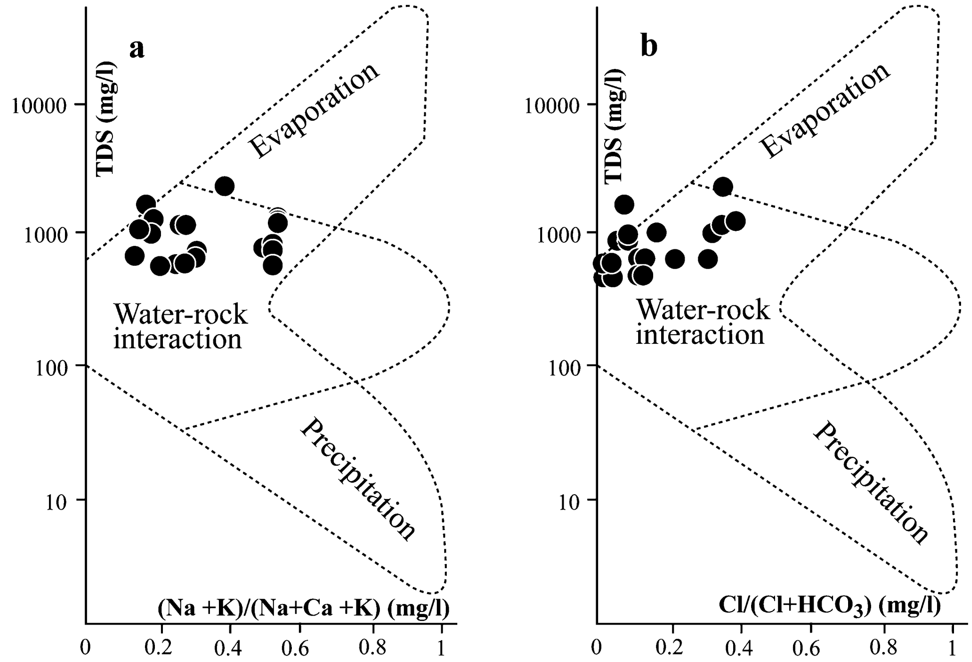

The major species in the waters were studied using stoichiometric relations among some solutes (Table 6), correlation diagrams (Fig. 10), and Pearson correlation analysis (Table 5). The corresponding ratio of (Ca^{2+} + Mg^{2+})/total cations of the samples is > 0.5 (0.51–0.85), suggesting a significant input of Ca^{2+} and Mg^{2+} in total cations of analyzed waters (Matini et al. 2012; Kamtchueng et al. 2016). Furthermore, in Fig. 10a, the plot of (Ca^{2+} + Mg^{2+}) versus total cations for the samples shows that the totality of the points was beneath the 1:1 line demonstrating the involvement of weathering process. This is sustained by the positive correlation observed between TDS with Mg^{2+}, Ca^{2+}, Na^+, and K^+ (r = 0.75, r = 0.88, r = 0.63, and r = 0.65, respectively).

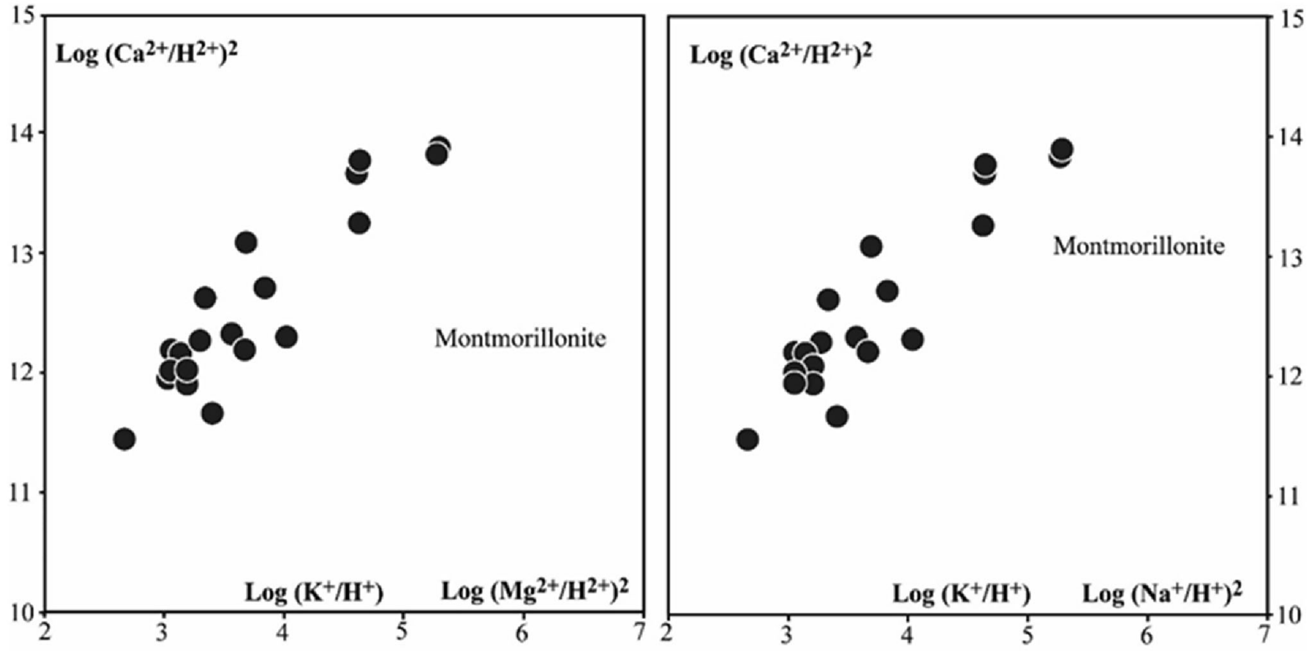

Fig. 9 Plots of various water samples in the Korjinski diagram (1948). This diagram was realized assuming a temperature of 25 °C and a pressure of 1 atm, using the DIAGRAMME computer program

Further, the scattering of points around the 1:1 line on the ($Mg^{2+} + Ca^{2+}$) versus ($SO_4^{2-} + HCO_3^-$) diagram (Fig. 10b) demonstrates that the input of Ca and Mg content in groundwater does not come from carbonated minerals dissolution (Matini et al. 2012; Kamtchueng et al. 2016). Nevertheless, the clustering of some points near this 1:1 line also indicates that in addition to silicates weathering, basic dissolution of carbonate minerals (like calcite included in some study area rocks presented in Fig. 10c, d may also contribute to the input of Ca^{2+} and Mg^{2+} in waters (Hounslow 1995). These results prove that silicate dissolution is the principal source of alkaline Earth metals in water samples.

The (K + Na)/total cations ratios of all samples are < 0.5 (with values fluctuating between 0.15 and 0.49) signifying also that dissolution of silicates minerals was the main source of major cations in groundwater of the Makabaï area (Srinivasamoorthy et al. 2008). The high Ca^{2+}, HCO_3^-, and Mg^{2+} concentrations in the waters, therefore, result from the reaction between the reactive silicate and the H_2CO_3.

As illustrated in Fig. 10e, the contents of Na^+ are not compensated by Cl^- as would be projected if aerosol inputs and/or seawater were the only source of Na^+, and the Na/Cl ratio is not reliable with a simple seawater/fresh (precipitation) mixing process. Hence, the plagioclase dissolution (albite or sodium feldspar which is the principal mineral phase in rock-thin sections) is probably the main geochemical process responsible for liberating additional Na into the solution, leading to Na/Cl ratios (1.14–13.26) (Table 6) superior to that of seawater (0.86) (Fisher and Mulican 1997). The ion interchange process is moreover confirmed by the Na/Ca ratio (0.15–1.15) and the scatter diagram of Na versus Ca (Fig. 10c), in which all water samples plotted under the 1:1 line (Srinivasamoorthy et al. 2008). The plagioclase dissolutions are thus not the only supplier of Na^+ ions surplus, but also the exchange between Na^+ and Ca^+ cations.

The ion interchange process can be checked in the chemistry of the studied water samples by the examination of the relationship between (Na − Cl) and (SO_{4} + HCO_3) − (Mg + Ca) (Fig. 10f). If ion interchange is a significant geochemical process governing the chemistry of the waters, the above relationship should be linear with a slope of − 1.0 (Fisher and Mulican 1997). Figure 10f indicated that data are more or less scattered around the line with a slope of about − 0.45 indicating that the ion exchange reaction was not a significant geochemical process controlling the chemistry of groundwater.

According to Fisher and Mulican (1997), normal ion exchange is moreover confirmed by an excess of ΣHCO_3 + SO_4 over ΣCa + Mg, whereas the reverse ion interchange is expressed by an excess of ΣCa + Mg over $\Sigma HCO_3 + SO_4$. On this basis, (Jankowski et al. 1998; Fantong et al. 2009 and Kumar et al. 2007) demonstrated that the process of ion exchange is defined as direct when K^+ or Na^+ in water is substituted by Mg^{2+} or Ca^{2+} from the rock, and as indirect when Mg^{2+} or Ca^{2+} is replaced by

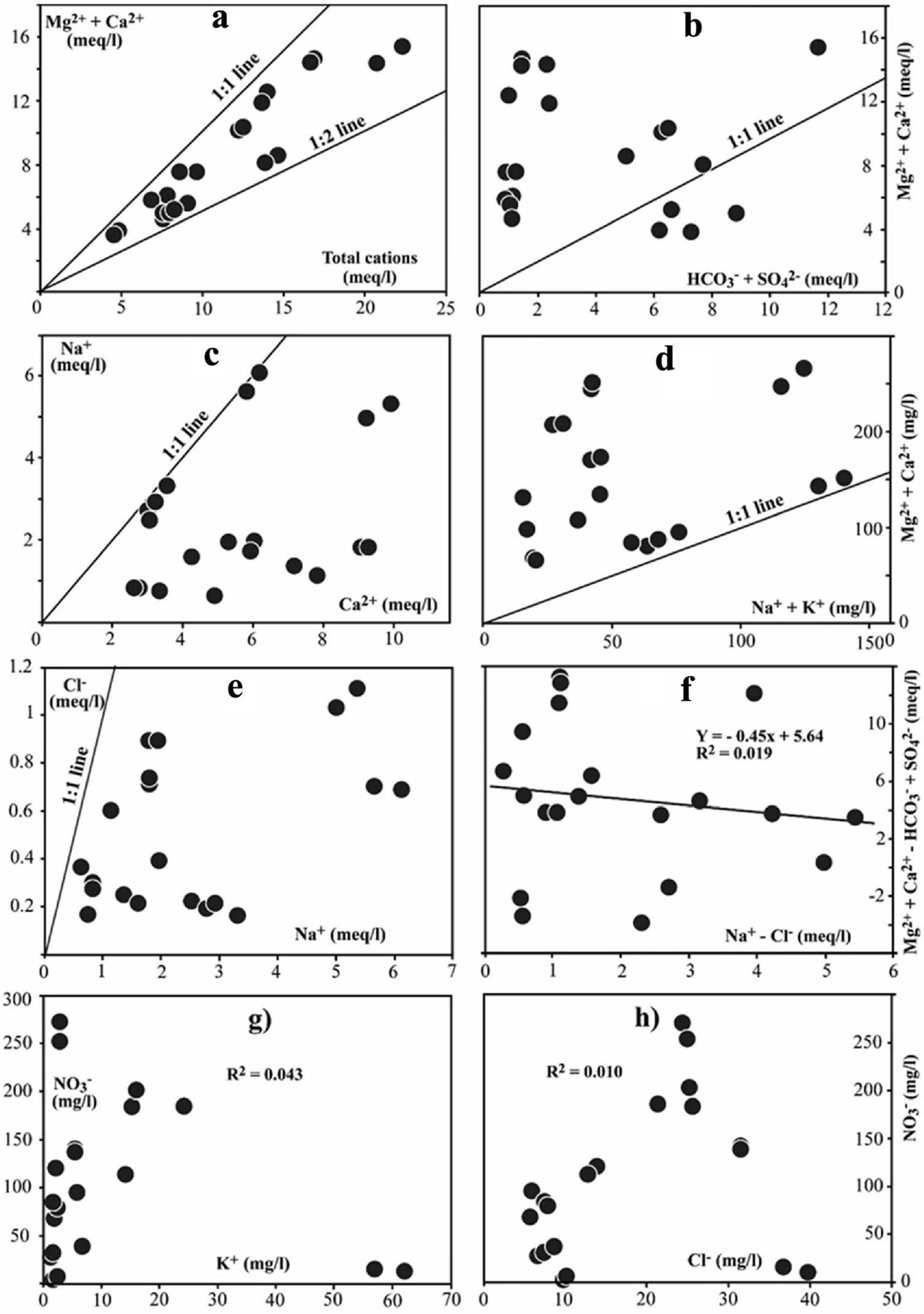

Fig. 10 Cross plots presenting the interrelationship among dissolved species: **a** (Mg^{2+} + Ca^{2+}) versus Total cations; **b** (Mg^{2+} +Ca^{2+}) versus (HCO_3^- +SO_4^{2-}); **c** Na^+ versus Ca^+; **d** (Mg^{2+} +Ca^{2+}) versus (Na^+ + K^+) diagram; **e** Na^+ versus Cl^-; f) (Mg^{2+} + Ca^{2+} − HCO_3^- + $SO4^{2-}$) versus (Na^+ − Cl^-); **g** (NO_3^- vs. K^+), **g** (NO_3^- vs. Cl^-)

K^+ or Na^+. The majority of samples (55%) display a Ca + Mg/HCO_3 + SO_4 ratio > 1, indicating the direct type of the base-exchange reaction, which implicates the liberation of Mg or Ca into groundwater and the adsorption of K or Na by clay minerals. To confirm this last statement, the plotting of the analyzed waters in the (Hendry and Wassenaar 2000) diagram (Fig. 10d) helps to apprehend the behavior of Ca^{2+}–Mg^{2+} and the K^+–Na^+ in the groundwater. All samples were plotted above the 1:1 equiline, showing that Mg^{2+} and Ca^{2+} are preferentially released into solution whereas there is adsorption of K^+ and Na^+ by clay minerals.

The nature of the ion interchange reaction can also be determined using the chloro-alkaline index (CAI) (Schoeller 1967; Jankowski et al. 1998). This index was calculated following the formula of (Schoeller 1967), where all values are in meq/L (Table 6). Chloro-alkaline disequilibrium or normal exchange between Mg^{2+} or Ca^{2+} in water with K^+ and Na^+ in the material of the aquifer indicates that CAI 1 and CAI 2 indices give negative

Table 5 Spearman's correlation coefficients for physicochemical parameters of groundwater samples

	pH	EC	TDS	AlK	TH	Na^+	NH^{4+}	K^+	Mg^{2+}	Ca^{2+}	F^-	Cl^-	NO_3^-	PO_4^{3-}	SO_4^{2-}	HCO_3^-
pH	**1**															
EC	*0.70	1														
TDS	*0.69	*1.00	1													
AlK	− 0.27	0.08	0.05	1												
TH	*0.79	*0.83	*0.85	− 0.25	1											
Na^+	0.13	*0.62	*0.63	0.35	0.24	1										
$NH4^+$	− 0.12	0.10	0.09	0.48	0.00	0.00	1									
K^+	*0.69	*0.64	*0.65	− 0.24	*0.86	− 0.02	0.22	1								
Mg^{2+}	*0.69	*0.73	*0.75	− 0.31	*0.95	0.12	0.13	*0.90	1							
Ca^{2+}	*0.82	*0.87	*0.88	− 0.25	*0.99	0.30	− 0.02	*0.85	*0.92	1						
F^-	0.06	*0.46	0.47	0.12	0.24	0.47	0.19	0.10	0.27	0.25	1					
Cl^-	*0.69	*0.77	*0.76	0.19	*0.77	0.26	0.25	*0.68	*0.69	*0.76	− 0.05	1				
NO_3^-	0.14	0.40	0.42	− 0.25	0.39	0.17	− 0.20	0.31	0.38	0.40	0.24	0.30	**1**			
PO_4^{3-}	− 0.16	− 0.32	− 0.38	0.30	− 0.38	− 0.26	0.06	− 0.34	− 0.38	− 0.38	− 0.38	− 0.10	− 0.38	**1**		
SO_4^{2-}	*0.61	*0.71	0.69	0.25	*0.59	0.38	0.15	*0.52	0.45	*0.63	− 0.11	*0.87	0.31	− 0.06	**1**	
HCO_3^-	**− 0.27**	0.08	0.05	*1.00	− 0.26	0.36	0.47	− 0.25	− 0.31	− 0.25	0.12	0.19	− 0.25	0.30	0.25	**1**

*Significant at $p < 0.05$

Table 6 Stoichiometric relations between some solutes in the water groundwater samples

Sample ID	(Ca + Mg)/Total cations	(Na + K)/Total cations	(Ca + Mg)/ HCO_3	(Ca + Mg)/ (HCO_3 + SO_4)	Na/ Cl	Na/ Ca	CAI1	CAI2
W1-1	0.52	0.48	0.35	0.31	5.23	1.14	− 7.47	0.21
W1-2	0.51	0.49	0.63	0.51	5.76	1.15	− 8.31	0.03
W2-3	0.59	0.41	3.51	1.99	3.13	0.62	− 5.20	− 1.53
W2-4	0.59	0.41	0.57	0.40	3.09	0.62	− 5.06	0.53
W3-5	0.55	0.45	2.27	1.66	13.26	1.08	− 20.57	− 1.43
W3-6	0.74	0.26	2.25	1.66	4.89	0.43	− 7.53	− 0.79
W4-7	0.81	0.19	6.09	3.17	1.63	0.23	− 2.33	0.22
W4-8	0.81	0.19	5.44	3.15	1.64	0.23	− 2.39	0.24
W5-9	0.80	0.20	4.60	1.65	1.23	0.17	− 2.32	0.28
W5-10	0.85	0.15	4.78	3.57	3.52	0.22	− 5.88	− 0.69
W6-11	0.81	0.18	4.46	2.73	1.14	0.15	− 2.38	− 0.01
W6-12	0.74	0.26	2.75	1.96	3.25	0.42	− 4.76	− 0.25
W7-13	0.55	0.45	1.77	1.29	9.44	1.08	− 14.54	− 1.62
W7-14	0.80	0.19	2.14	1.83	2.85	0.26	− 5.11	− 0.19
W8-15	0.77	0.23	0.50	0.45	1.44	0.37	− 1.49	0.65
W8-16	0.78	0.21	0.51	0.46	1.31	0.34	− 1.28	0.66
W9-17	0.76	0.23	0.20	0.19	1.85	0.35	− 2.73	0.15
W9-18	0.76	0.23	0.16	0.16	1.96	0.35	− 2.90	0.16
W10-19	0.58	0.41	0.16	0.16	7.35	0.96	− 11.40	− 0.03
W10-20	0.55	0.44	0.23	0.22	8.90	1.07	− 13.72	− 0.16
Minimum	0.51	0.15	0.16	0.16	1.14	0.15	− 20.57	− 1.62
Maximum	0.85	0.49	6.09	3.57	13.26	1.15	− 1.28	0.66
Mean	0.69	0.3	2.26	1.42	4.42	0.57	− 6.78	− 0.21
SD	0.12	0.12	2	1.13	3.32	0.37	5.14	0.69

CAI chloro-alkaline index [CAI 1 = $Cl^- - (Na^+ + K^+)/Cl^-$, CAI 2 = $Cl^- - (Na^+ + K^+)/(HCO_{3-} + SO_4^{2-} + NO_3^{2-}$, where all values are expressed in meq/L]; *SD* standard deviation

values. When there is chloro-alkaline equilibrium or reverse ion interchange between K^+ and Na^+ in water with Mg^{2+} or Ca^{2+} in the matrix of the aquifer system, then these indices will give positive values (Schoeller 1967; Gupta et al. 2009). The great majority of analyzed samples display negative values of CAI signifying that normal ion exchange predominated over reverse ion interchange. Therefore, in addition to the minerals weathering included in the country rocks represented by mugearite, hawaiite, and basalt lavas, base-exchange reactions also play a significant role in changing the geochemistry of groundwater composition.

4.3.2 *Anthropogenic origin*

Explanation of disparities in the geochemistry of groundwater due to interference of human being activities is a very complex task. Irrigation return flow, for instance, is a source of Mg^{2+}, Ca^{2+}, Na^+, SO_4^{2-}, HCO_3^-, and Cl^- of the semiarid and arid regions. Na^+, Mg^{2+}, K^+, SO_4^{2-}, NO_3^-, F^- and Cl^-, are commonly recognized as pollutants from the application of agrochemicals (phosphate, nitrogen, potash, and sulfate fertilizers), septic tanks leakage, domestic waters outflow and livestock areas (Todd 1980; Subba et al. 2012a; Sadek Awad 2011; Li et al. 2016). The other source of Ca^{2+} is the lime [$Ca(OH_2)$] used in cement, which is a material for constructional activities (Somasundaram et al. 1993; Subba Rao et al. 2005; Jiang et al. 2009). These factors increase the concentrations of chemical composition in the water of aquifer systems formed by geogenic origin.

Table 5 presents the Pearson's correlation results of physico-chemical parameters of assessed waters samples. The results revealed approximately 17%, 13%, and 68% of the physico-chemical parameters to be strongly ($r \geq 0.7$), moderate ($0.5 < r < 0.7$), and poorly ($r < 0.5$) based on the classification of (Saleem et al. 2012). However, we note two perfect values and a zero value respectively for the elements EC and TDS, Alk and HCO_3^-, and Na^+ and NH_4^+. At $p < 0.05$, parameters that correlated strongly with one another include: pH with EC (r = 0.70), TDS (r = 0.69), TH (r = 0.79), K^+ (r = 0,69), Mg^{2+} (r = 0.69), Ca^{2+} (r = 0.82), Cl^- (r = 0.69); EC with TDS (r = 1), TH (r = 0.83), Mg^{2+} (r = 0.73), Ca^{2+} (r = 0.87), Cl^- (r = 0.77), SO_4^{2-} (r = 0.71); TDS with TH ((r = 0.85), Mg^{2+} (r = 0.75), Ca^{2+} (r = 0.88), Cl^- (r = 0.76); Alk with HCO_3^- (r = 1); TH with K^+ (r = 0.86), Mg^{2+} (r = 0.95), Ca^{2+} (r = 0.99), Cl^- (r = 0.77); K^+ with Mg^{2+} (r = 0.90), Ca^{2+} (r = 0.85); Mg^{2+} with Ca^{2+} (r = 0.92); Ca^{2+} with Cl^- (r = 0.76); Cl^- with SO_4^{2-} (r = 0.87). The weak positive correlation of SO_4^{2-} with HCO_3^- and Mg^{2+} ($r = 0.25$ and $r = 0.45$) suggests that weathering of rock-forming minerals is not the main source that accounts for SO_4^{2-} concentration in the solution. On the other hand, SO_4^{2-} with Ca^{2+} and K^+ correlate positively ($r = 0.63$ and $r = 0.52$ respectively) and F^- with Ca^{2+}, Mg^{2+}, K^+, Na^+ and Cl^- display no significant correlation ($r = 0.25$, $r = 0.27$, $r = 0.1$, $r = 0.47$ and $r = -0.05$ respectively) (Table 5). These observations indicate the predominance of anthropogenic contributions as like household wastes, coal combustion, or sulfate fertilizers (Sadek Awad 2011) for SO_4^{2-} and over natural enrichment for F^- in Makabaï area groundwater (Jha et al. 2011; Kamtchueng et al. 2016). Fluor-apatite and micas in the granites were identified as the main provenance of fluoride in the groundwater through water–rock interactions in an alkaline medium (Fantong et al. 2009). It is important to note that whether it is human pollution or a natural origin of these different elements, the contents of SO_4^{2-} and F^- in the analyzed samples are lower than the 2004 standard authorized by the WHO. In the Makabaï area, sanitary facilities are very poor, and constructional and agricultural activities are frequent. Thus, the anthropogenic contributions comprising irrigation return flow, chemical fertilizers, constructional activities, and wastewater effluents can also control groundwater chemistry. To clarify the incidence of anthropogenic actions in aquifer systems, the studies linked to TDS with other ions can be taken into account because all chemical parameters contribute to TDS. In addition to geogenic origin of sampled water, the positive correlation observed between TDS with major cations K^+, Mg^{2+}, Ca^{2+}, Na^+ (r = 0.65, r = 0.75, r = 0.88, and r = 0.63, respectively) and with anions Cl^-, F^- and NO_3^- comforts the impacts of anthropogenic activities inputs.

In the natural environment, NO_3 is a highly mobile anion and is soluble in water (Hem 1989). According to (Panno et al. 2001; Tamma Rao et al. 2013), NO_3 is found naturally at low contents in precipitation but is frequently enriched to high levels by anthropogenic activities. In the Makabaï area, 90% of analyzed waters have nitrate contents above the WHO standard. To understand the anthropogenic source of extra NO_3 in the solution, the relationship between NO_3^- and K^+ and between NO_3^- and Cl^- have been studied. Since, NO_3^- displayed insignificant correlation with major cations (K^+: $r = 0.31$, Na^+: $r = 0.17$, Mg^{2+}: $r = 0.38$, Ca^{2+}: $r = 0.40$) and Cl^- ($r = 0.30$), and no linear relation was found between NO_3^- versus K^+ and NO_3^- versus Cl^- (Fig. 10g, h), it can be deduced that NO_3 and Cl in the Makabaï area originate from different sources. It also indicates negligible contamination of groundwater by human-related activities. The NO_3^- presence in this zone is largely related to oxidation–reduction reactions of organic matter associated with septic-tank effluent and animal waste intense production (Huneau et al. 2011; Bello et al. 2019). It is important to note that in this area, there is intense livestock production with a real cohabitation between the populations and the herds of cattle whose enclosures are sometimes located in the concessions. These observations are similar to earlier studies (Kamtchueng et al. 2014, 2016; Wirmvem et al. 2013; Wakida and Lerner 2005; Barakat et al. 2018) on groundwater in Nottingham city in England, and in Ndop plains, Monoun and Nyos in Cameroon respectively, where spreading of animal manure and urine, sewage sludge, effluent, and agricultural use were inferred as the plausible causes of increased levels of NO_3 in the aquifer system.

4.4 Hierarchical cluster analysis

When numerous measurements (hydrochemical data such as TDS, EC, pH, Mg^{2+}, and NO_3^-, considered as variables) are completed on each individual or object in one or more samples, the hierarchical cluster analysis (HCA) technique can be applied (Rencher 2002; Shawgar et al. 2020). The preliminary step of HCA is to seek the dissimilarity or similarity among every couple of objects in the dataset. The next step consists to group the objects into a dendrogram (also called a hierarchical cluster tree). Hydrochemical variables measured in this study comprising, EC, pH, TDS, Mg^{2+}, Ca^{2+}, K^+, Na^+, HCO_3^-, NO_3^-, Cl^-, and SO_4^{2-}, were used for this analysis which yields a dendrogram. Figure 11 shows the Dendrogram with the hierarchical clusters of analyzed samples site (a) and the hierarchical clusters of analyzed parameters (b). The hierarchical cluster tree grouped 20 water samples into four statistically major groups (or clusters) (Fig. 11a). This grouping could be explained by the nature of the permeable formations where these waters can be stored. This explanation is verifiable in the field, where from one well to another and practically in the same place, the quality of water can vary considerably. This reflects the complexity of the functioning of underground and surface hydro-systems from the point of view of water quality and the need to consider them even at the scale of a small hydrogeological unit as a mosaic of small systems independent of each other. This complexity has been also highlighted by

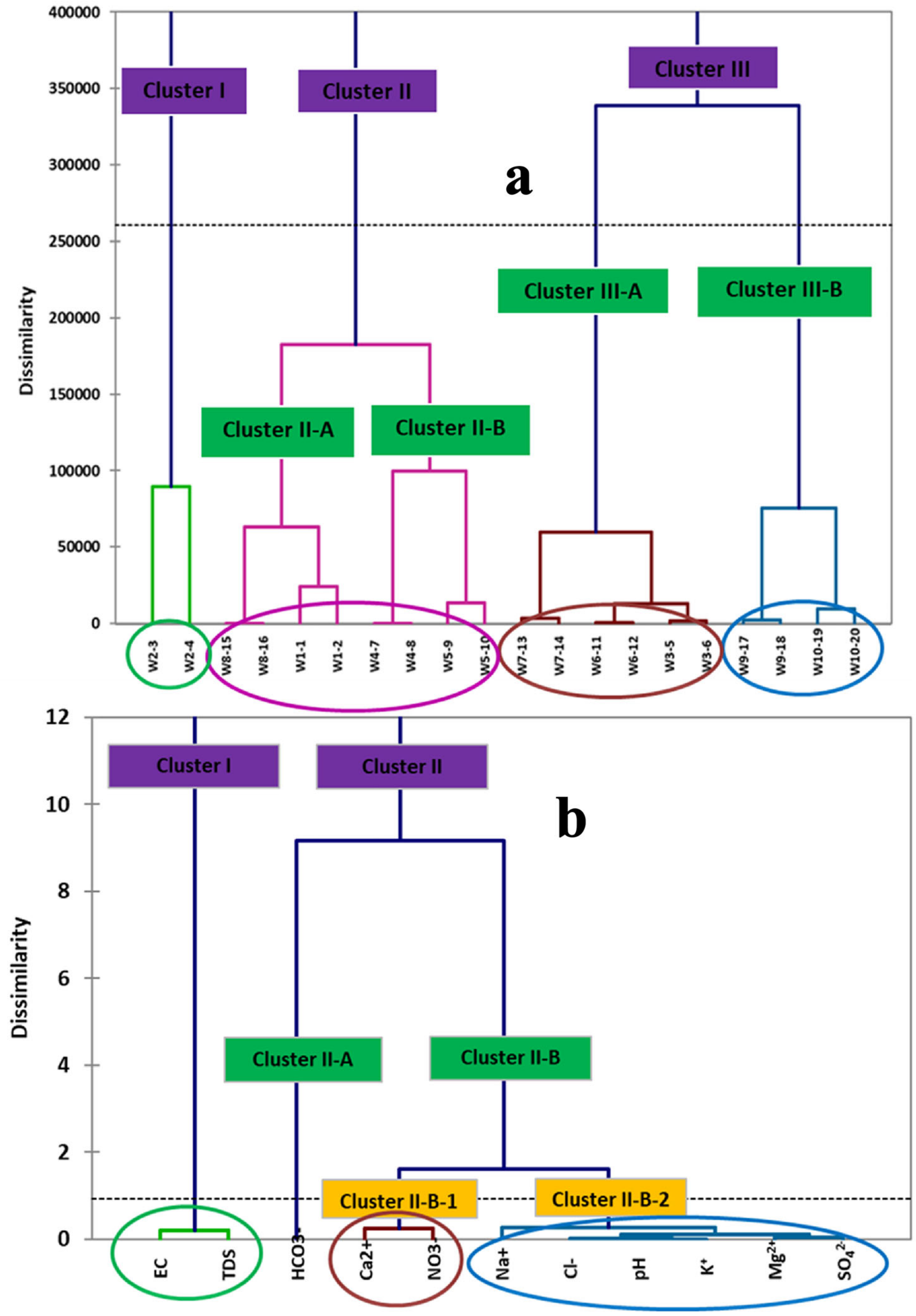

Fig. 11 Dendrogram showing the hierarchical clusters of analyzed samples site (**a**) and the hierarchical clusters of analyzed parameters (**b**)

Dewandel et al. 2006, 2011; Mfonka et al. 2019 and Kemgang 2019 using hydrodynamic characteristics of the aquifer (piezometric fluctuation, spherical variographic model, hydraulic conductivity, storage capacity of the piezometers, local structure of the aquifer, initial state of the aquifer, topography and geophysics methods). Figure 11b shows two large groupings of ions. Although these groupings are identified, they do not respect a perfect logic of association. So, the ions NO_3^- and Cl^- concentrations of anthropogenic pollutants appear to be a major distinguishing factor. However, the water quality of the study area is influenced by two main factors: the nature of the geological substratum by hydrolysis of minerals and rocks, the leaching of the soil, and to a lesser extent an anthropogenic origin (low level of sanitation, lack of hygiene culture…) (Zghibi et al. 2014; Chihi et al. 2015; Xiao et al. 2015; Liguang et al. 2015; Menció et al. 2016; Ramesh et al. 2018; Jiutan et al. 2019).

5 Conclusion

The current study has been conducted to evaluate the chemistry of bedrocks in the crystalline basement of Mount Makabaï (Maroua-Cameroon city) in relation to the groundwater geochemistry in the investigated area. The petrography and geochemistry of geologic formations, morphological characteristics of weathering material, and physicochemical characteristics of soil solutions and water samples can be summarized as follows:

(1) Bedrocks exhibit porphyritic, aphyric, and subaphiric textures. They are mainly constituted of olivine, clinopyroxene, plagioclase, calcite, and oxides. Based on whole rock major element chemical compositions, the Makabaï samples, plotted on $Na_2O + K_2O$ versus SiO_2 diagram range in composition from basalt and hawaiite to mugearite. The ratio of the sum of the alkaline Earth metals over the alkali metals $(MgO + CaO)/(Na_2O + K_2O)$ exceeds unity and shows dominance of alkaline Earth metals (MgO: 2.99–4.48 %; CaO: 6.19–9.80 %) in relation to alkali metals (Na_2O: 2.27–4.46 %; K_2O: 2.09–2.51 %);

(2) Exchangeable bases contents are high, mostly represented by Ca^{2+} and Mg^{2+}, whose contents vary from 14.6 to 35.28 cmol(+) kg^{-1} and from 3.28 to 9.48 cmol(+) kg^{-1} corresponds to mean values of 24.42 ± 8.70 and 6.22 ± 2.84 cmol(+) kg^{-1} respectively. The CEC_{clay} is also high, ranging between 116.80 and 181.38 cmol(+) kg^{-1}, values in line with the presence of 2:1 clay minerals represented in the study area by montmorillonite;

(3) Hydro-geochemical classification by using Piper trilinear diagram revealed two water types in the study sites: (1) CaMg–HCO_3 (40 %) and (2) CaMg–Cl or CaMg–SO_4 (60 %). The composition of dissolved ions in groundwater is controlled by weathering of olivine, clinopyroxene, plagioclase, calcite, and oxides found in host rocks. The similarity in the trend of cations and anions in groundwater and oxides in rocks and soil samples suggests the influences of local rock and soil chemistry on the groundwater chemistry and hence, water–rock interaction observed in the study area. The majority of samples (55 %) of the samples display a $Ca + Mg/HCO_3 + SO_4$ ratio > 1, indicating the direct type of the base-exchange reaction, which implicates the liberation of Mg^{2+} or Ca^{2+} into groundwater and adsorption of K^+ or Na by clays minerals;

(4) The observations indicate the predominance of anthropogenic contributions like household wastes, coal combustion, and sulfate fertilizers for SO_4^{2-} and over natural enrichment for F^- in groundwater of the Makabaï area.

Acknowledgements We are grateful to anonymous referees for their constructive critics and suggestions which substantially improved the quality and standard of the manuscript.

Funding Not applicable.

Declarations

Conflict of interest On behalf of all authors, the corresponding author states that there is no conflict of interest.

References

Adabanija MA, Afolabi OA, Lawal L (2019) The influence of bedrocks on groundwater chemistry in a crystalline basement complex of southwestern Nigeria. Environ Earth Sci 79:87

Adeli M, Mohammadi Z, Keshavarzi B, Keyvan Amjadian K, Kafi M (2021) Heavy metal(loid) pollution of a hard-rock aquifer: evidence, distribution, and source. Environ Sci Pollut Res. https://doi.org/10.1007/s11356-021-13079-2

Ako Ako A, Shimada J, Hosono T, Ichiyanagi K, Nkeng GE, Fantong WY, Takem GEE, Njila NR (2011) Evaluation of groundwater quality and its suitability for drinking, domestic, and agricultural uses in the Banana Plain (Mbanga, Njombe, Penja) of the Cameroon Volcanic Line. Environ Geochem Health 33:559–575

Ako Ako A, Shimada J, Hosono T, Kagabu M, Ayuk AR, Nkeng GE, Takem GEE, Takounjou ALF (2012) Spring water quality and usability in the Mount Cameroon area revealed by hydrogeochemistry. Environ Geochem Health 34(5):615–639. https://doi.org/10.1007/s10653-012-9453-3

An TD, Tsujimura M, Le-Phu V, Kawachi A, Ha DT (2014) Chemical characteristics of surface water and groundwater in coastal watershed, Mekong Delta, Vietnam. Procedia Environ Sci 20:712–721

Appelo CAJ, Postma D (2004) Geochemistry, groundwater and pollution, 2nd edn. CRC press, Florida

Awad S (2011) Hydrochimie et faciès géochimiques des eaux souterraines, Plaine De Bekaa. Hydrol Sci J 56(2):334–348. https://doi.org/10.1080/02626667.2011.559331

Baise D, Jabiol B (1995) Guide pour la Description des Sols. Institut National de la Recherche Agronomique (INRA), Paris

Barakat A, Meddah R, Afdali M, Touhami F (2018) Physicochemical and microbial assessment of spring water quality for drinking supply in Piedmont of Béni-Mellal Atlas (Morocco). Phys Chem Earth Parts a/b/c 104:39–46

Bello M, Ketchemen Tandia B, Nlend B, Huneau F, Fouepe A, Fantong WY, Ngo Boum Nkot S, Garel E, Celle Jeanton H (2019) Shallow groundwater quality evolution after 20 years of exploitation in the southern Lake Chad: hydrochemistry and stable isotopes survey in the far north of Cameroon. Environ Earth Sci 78:474

Bodrud-Doza M, Towfiqul Islam ARM, Ahmed F, Das S, Saha N, Safiur Rahman M (2016) Characterization of groundwater quality using water evaluation indices, multivariate statistics and geostatistics in central Bangladesh. Water Sci 30(1):19–40

Boronina A, Ramillien G (2008) Application of AVHRR imagery and GRACE measurements for calculation of actual evapotranspiration over the Quaternary aquifer (Lake Chad basin) and validation of groundwater models. J Hydrol 348(1–2):98–109

Bouyo MH, Zhao Y, Penaye J, Zhang SH, Njel UO (2015) Neoproterozoic subduction-related metavolcanic and metasedimentary rocks from the Rey Bouba Greenstone Belt of north-central Cameroon in the Central African Fold Belt: new insights into a continental arc geodynamic setting. Precambrian Res 261:40–53

Bouyo Houketchang M, Toteu SF, Deloule E, Penaye J, Van Schmus WR (2009) U-Pb and Sm–Nd dating of high-pressure granulites from Tcholliré and Banyoregions: evidence for a Pan-African granulite facies metamorphism in north-central Cameroon. J Afr Earth Sci 54:144–154

Brindha K, Kavitha R (2015) Hydrochemical assessment of surface water and groundwater quality along Uyyakondan channel, south India. Environ Earth Sci 73:5383–5393

BUCREP (2011) Rapport national sur l'état de la population: Enjeux et défis d'une population de 20 millions d'habitants au Cameroun en 2011

Candela L, Elorza FJ, Tamoh K, Jiménez-Martínez J, Aureli A (2014) Groundwater modelling with limited data sets: the Chari-Logone area (Lake Chad Basin, Chad). Hydrol Process 28(11):3714–3727

Cheo EA, Voigta HJ, Wendland F (2017) Modeling groundwater recharge through rainfall in the Far-North region of Cameroon. Groundw Sustain Dev 5:118–130

Chihi H, de Marsily BH, Yahyaoui H (2015) Relationship between tectonic structures and hydrogeochemical compartmentalization in aquifers: example of the "Jeffara de Medenine" system, south-east Tunisia. J Hydrol Reg Stud 4:410–430

Derron MH (1999) Interaction eau-roche de basse température: géochimie des métaux dans l'altération météorique des roches mafiques alpines. Thèse Doct Fac Sci Univ. Lausanne 128

Dewandel B, Lachassagne P, Wyns R, Marechal JC, Krishnamurthy NS (2006) A generalized 3-D geological and hydrogeological conceptual model of granite aquifers controlled by single or multiphase weathering. J Hydrol 330:260–284

Dewandel B, Lachassagne P, Zaidi FK, Chandra S (2011) A conceptual hydrodynamic model of a geological discontinuity in hard rock aquifers: example of a quartz reef in granitic terrain in South India. J Hydrol 405:474–487

Djao R, Kaoussiri B, Abouna M, Achili MA (2011) Guide pratique de la gestion d'une épidémie de choléra. Ministère de la Santé Publique/SNV Cameroun

Djaouda M, Njiné T, Liang S, Ebang Menye D, Gaké B, Zébazé Togouet SH, Nola M (2014) Bacteriological quality of well waters in Garoua, North Cameroon. Water Qual Expo Hea 6:161–176

Djeuda THB (1987) Géologie et hydrogéologie d'un secteur de la zone mobile d'Afrique Centrale: région de poli, Nord Cameroun. Doctoral dissertation, Université Scientifique et Médicale de Grenoble. p 304+annexes

Domenico PA, Schwartz FW (1998) Physical and chemical hydrogeology, 2nd edn. Wiley, New York, p 506

Eshtawi T, Evers M, Tischbein B (2016) Quantifying the impact of urban area expansion on groundwater recharge and surface runoff. Int Assoc Sci Hydrol Bull 61(5):826–843

Faniran JA, Ngceba FS, Bhat RB, Oche CY (2001) An assessment of the water quality of the Isinuka springs in the Transkei region of the Eastern Cape. Repub S Afr Water SA 27(2):241–250

Fantong WY, Satake H, Ayonghe SN, Aka FT, Kazuyoshi A (2009) Hydrogeochemical controls and usability of groundwater in the semi-arid Mayo Tsanaga River Basin: Far north province, Cameroon. Environ Geol 58:1281–1293

Fantong WY, Satake H, Ayonghe SN, Suh CE, Adelana SMA, Fantong EBS, Banseka HS, Gwanfogbe CD, Woincham LN, Uehara Y, Zhang J (2010) Geochemical provenance and spatial distribution of fluoride in groundwater of Mayo Tsanaga River Basin, Far north Region, Cameroon: implications for incidence of fluorosis and optimal consumption dose. Environ Geochem Health 32:147–163

Fantong WY, Kamtchueng BT, Ishizaki Y, Chi Fru E, Bi Fantong E, Wirmvem MJ, Aka FT, Nlenda B, Harman D, Uedae A, Kusakabe M, Tanyileke G, Ohba T (2019) Major ions, δ^{18}O, δ^{13}C and ^{87}Sr/^{86}Sr compositions of water and precipitates from springs along the Cameroon volcanic line (Cameroon, west Africa): Implications for provenance and volcanic hazards. J Afr Earth Sci 150:12–22

Fisher RS, Mulican WFIII (1997) Hydrochemical evolution of sodium-sulfate and sodium-chloride groundwater beneath the Northern Chihuahuan Desert, Trans-Pecos, Rexas, USA. Hydrogeol J 10:455–474

Furry V (1997) Les eaux souterraines en Picardie. Mém. D.E.S.S. Environnement, Univ. Picardie Jules Verne. p 30+annexes

Ganyaglo SY, Benoeng-Yakubo B, Osae S, Dampare SB, Fianko JR, Bhuiyan MAH (2010) Hydrochemical and isotopic characterization of groundwaters in the eastern region of Ghana. J Water Resour Prot 2:199–208

Garrels RM (1976) A survey of low temperature water mineral relations, in interpretation of environmental isotope and hydrogeochemical data in groundwater hydrology, Vienna. International Atomic Energy Agency. pp 65–84

Gastmans D, Chang HK, Hutcheon I (2010) Groundwater geochemical evolution in the northern portion of the guarani aquifer system (Brazil) and its relationship to diagenetic features. Appl Geochem 25:16–33

Gibbs RJ (1970) Mechanisms controlling world water chemistry. Science 17:1088–1090

Gountié Dedzo M, Tsozué D, Mumbfu Mimba E, Teddy F, Mofor Nembungwe R, Linida S (2017) Importance of rocks and their weathering products on groundwater quality in central-east Cameroon. Hydrology 4:1–18

Gupta S, Dandele PS, Verma MB, Maithani PB (2009) Geochemical assessment of groundwater around Macherla- Karempudi area, Guntur District. Andhara Pradesh J Geol Soc India 73:202–212

Hambaté GV, Essomba NS, Ombolo A, Loura B (2015) Bacteriological and physicochemical characterization of water from wells in urban areas of the District of Maroua III (Far North Cameroon). Int J Curr Trends Eng Technol 1(2):43–50

Hanrion C (1976) Techniques used for the preparation of petrographic thin sections. Laboratoire commun de pétrographie-minéralogie ORSTOM: Adiopodoumé-Côte d'Ivoire

Hem HD (1989) Study and interpretation of the chemical characteristics of natural waters, 3rd edn. U.S. Geological Survey Water-Supply. p 2254

Hendry MJ, Wassenaar LL (2000) Controls on the distribution of majors ions in pore waters of a thick surficial aquitard. Water Resour Res 36:503–513

Hounslow AW (1995) Water quality data: analysis and interpretation. Lewis Publishers, Boca Raton, FL, p 416

Huneau F, Dakoure D, Celle-Jeanton H, Vitvar T, Ito M, Traore S, Compaore NF, Jirakova H, Le Coustumer P (2011) Flow pattern and residence time of groundwater within the south-eastern Taoudeni sedimentary basin (Burkina Faso, Mali). J Hydrol 409:423–439

Irvine TN, Baragar WRA (1971) A guide to the chemical classification of the common volcanic rocks. Can J Earth Sci 8:523–548

Jankowski J, Acworth RI, Shekarforoush S (1998) Reverse ionexchange in deeply weathered porphyritic dacite fractured aquifer system, Yass, New South Wales, Austria. In: Arehart GB, Hulston JR (eds) Proceedings of 9th international symposium on water–rock interaction, Balkema, Rotterdam. pp 243–246

Jha SK, Mishra VK, Sharma DK, Damodaran T (2011) Fluoride in the environment and its metabolism in humans. Rev Environ Contam Toxicol 211:121–142

Jiang Y, Wu Y, Groves Ch, Yun D, Kambesis P (2009) Natural and anthropogenic factors affecting the groundwater quality in the Nandong Karst underground river system in Yunan, Vhina. J Contamin Hydrol 109:49–61

Jiutan L, Jianguo F, Zongjun G, Min W, Guiheng L, Mengjie S, Hongying Z (2019) Hydrochemical characteristics and quality assessment of groundwater for drinking and irrigation purposes in the Futuan River Basin, China. Arab J Geosci 12:560

Kamtchueng BT, Fantong WY, Ueda A, Tiodjio ER, Anazawa K, Wirmvem MJ, Mvondo JO, Nkamdjou SL, Kusakabe M, Ohba T, Tanyileke G, Hell JV (2014) Assessment of shallow groundwater in Lake Nyos catchment (Cameroon, Central-Africa): implications for hydrogeochemical controls and uses. Environ Earth Sci 72:3663–3678

Kamtchueng BT, Fantong WY, Wirmvem MJ, Tiodjio RE, Takounjou AF, Ndam Ngoupayou JR, Kusakabe M, Zhang J, Ohba T, Tanyileke G, Hell JV, Ueda A (2016) Hydrogeochemistry and quality of surface water and groundwater in the vicinity of Lake Monoun, West Cameroon: approach from multivariate statistical analysis and stable isotopic characterization. Environ Monit Assess 524:1–24

Kemgang DT (2019) Etude hydrgéophysique de l'aquifère du quaternaire dans le bassin du lac Tchad par les méthodes RMP et TDEM: Extrême-Nord du Cameroun (plaine de piedmonts). Ph/D Thesis University of Ngaoundéré Cameroon. pp 209

Ketchemen B (1992) Étude hydrogéologie du Grand Yaéré (Extrême-Nord du Cameroun), synthèse hydrogéologique et étude de la recharge par les isotopes de l'environnement. Thèse Doctorat. Univ. de Dakar, Sénégal. p 172

Ketchemen-Tandia B, Boum-Nkot SN, Ebondji SR, Nlend BY, Emvoutou H, Nzegue O (2017) Factors influencing the shallow groundwater quality in four districts with different characteristics in urban area (Douala, Cameroon). J Geosci Environ Protect 5:99–120. https://doi.org/10.4236/gep.2017.58010

Khashogji MS, El Maghraby MMS (2013) Evaluation of groundwater resources for drinking and agricultural purposes, Abar Al Mashi area, south Al Madinah Al Munawarah City. Saudi Arab Arab J Geosci 6(10):3929–3942

Khazaei E, Mackay R, Warner JW (2004) The effects of urbanization on groundwater quantity and quality in the zahedan aquifer, southeast Iran. Water Int 29(2):178–188

Korjinski D (1948) Differential mobility of component of metasomatic zoning in metamorphism. In Proceedings of the 18th international geology congress, London, UK, pp. 5–7

Kristin S, Djoret D, Aminu MB, Sara V (2014) Études de la qualité des eaux souterraines dans la plaine d'inondation du Logone inférieur en avril-mai 2013. Projet Gestion Durable des eaux du Lac-Tchad. Rapport technique (7):48

Kumar M, Kumari K, Ramanathan A, Saxena R (2007) A comparative evaluation of groundwater suitability for irrigation and drinking purposes in two intensively cultivated districts of Punjab. India J Environ Geol 53:553–574

Kurdehlachin S, Jafari H, Bagheri R (2018) Geochemistry of groundwater from a rhyolite aquifer. Northwest Iran Environ Earth Sci 77:704

L'hote Y (2000) Climatologie. In: Atlas de la province de l'Etrême-Nord Cameroun (eds). Seignobos et Iyebi-Mandjek IRD. MINREST, Paris. pp 27–33

Langmuir D (1997) Aqueous environmental chemistry. Prentice Hall, New Jersey, p 600

Le Bas MJ, Le Maitre RN, Streckeisen A, Zanettin B (1986) A chemical classification of volcanic rock based on total silica diagram. J Pet 27:745–750

Leblanc M, Favreau G, Tweed S, Leduc C, Razack M, Mofor L (2007) Remote sensing for groundwater modelling in large semiarid areas: Lake Chad Basin, Africa. Hydrogeol J 15:97–100

Li P, Wu J, Qian H, Zhang Y, Yang N, Jing L, Yu P (2016) Hydrogeochemical characterization of groundwater in and around a wastewater irrigated forest in the southeastern edge of the Tengger Desert, Northwest China. Expo Health 8:331–348

Li P, He X, Li Y, Xiang G (2018) Occurrence and health implication of fluoride in groundwater of loess aquifers in the Chinese Loess Plateau: a case study of Tongchuan, northwest China. Expo Health. https://doi.org/10.1007/s12403-018-0278-x

Liguang J, Zhijun Y, Zhaofei L, Rui W, Shanshan W (2015) Hydrochemistry and its controlling factors of rivers in the source region of the Yangtze River on the Tibetan Plateau. J Geochem Explor 155:76–83

Ma FS, Wei AH, Deng QH, Zhao HJ (2014) Hydrochemical characteristics and the suitability of groundwater in the coastal region of Tangshan. China J Asian Earth Sci 25(06):1067–1075

Martin del Campo MA, Esteller MV, Expósito JL, Hirata R (2014) Impacts of urbanization on groundwater hydrodynamics and hydrochemistry of the Toluca Valley aquifer (Mexico). Environ Monit Assess 186:2979–2999

Matini L, Tathy C, Moutou JM (2012) Seasonal groundwater quality variation in Brazzaville, Congo. Res J Chem Sci 2:7–14

Mazor E (2004) Chemical and Isotopic groundwater hydrology. Marcel Dekker, New York

Mbawala A, Abdou A, Ngassoum MB (2010) Evaluation de la pollution physico-chimique et microbienne des eaux de puits de Dang-Ngaoundéré (Cameroun). Int J Biol Chem Sci 4(6):1962–1975

Menció A, Mas-Pla J, Otero N, Regàs O, Boy-Roura M, Puig R, Bach J, Domènech C, Zamorano M, Brusi D, Folch A (2016) Nitrate pollution of groundwater; all right…, but nothing else? Sci Total Environ 539:241–251

Mfonka Z, Ndam Ngoupayou JR, Kpoumié A, Ndjigui P-D, Zammouri M, Ngouh AN, Mouncherou OF, Mfochivé OF, Rakotondrabe F (2019) Hydrodynamic and groundwater vulnerability assessment of the shallow aquifer of the Foumban locality (Bamoun plateau, Western-Cameroon). Arab J Geosci 12:165. https://doi.org/10.1007/s12517-019-4328-x

Ngako V (1999) Les déformations continentales panafricaines en Afrique centrale: résultat d'un poinçonnement de type himalayen. Doctorate of the University of Yaoundé. pp 301

Ngounou NB (1993) Hydrogéologie d'aquifères complexes en zone semi-aride: les aquifères quaternaires du Grand Yaéré, Nord Cameroun. Thèse de doctorat, Univ. de Grenoble. p 352

Nguetnkam JP, Kamga R, Villiéras F, Ekodeck GE, Yvon J (2008) Variable weathering response of granite in tropical zones. Example of two sequences studied in Cameroon (Central Africa). C R Geosci 340:451–461

Nguetnkam JP, Villiéras F, Kamga R, Ekodeck GE, Yvon J (2014) Mineralogy and geochemical behavior during weathering of greenstone belt under tropical dry conditions in the extreme North Cameroon (Central Africa). Chem Erde-Geochem 74:185–193

Njel UO (1986) Paléogéographie d'un segment de l'orogenèse panafricaine: la ceinture volcano-sédimentaire de Poli (Nord Cameroun). C R Acad Sci Paris 303:1737–1742

Njitchoua R, Ngounou-Ngatcha B (1997) Hydrogeochemistry and environmental isotopes investigations of the north Diamare plain northern Cameroon. J Afr Earth Sci 25:307–316

Panno SV, Hackley KC, Hwang HH, Kelly WR (2001) Determination of the source of nitrate contamination in karst springs using isotopic and chemicals indicators. Chem Geol 179:113–128

Patel AK, Das N, Kumar M (2019) Multilayer arsenic mobilization and multimetal co-enrichment in the alluvium (Brahmaputra) plains of India: a tale of redox domination along the depth. Chemosphere 224:140–150

Penaye J, Kröner A, Toteu SF, Van Schmus WR, Doumnang JC (2006) Evolution of the Mayo-Kebbi region as revealed by zircon dating: an early (ca. 740 Ma) Pan-African magmatic arc in southwestern Chad. J Afr Earth Sci 44:530–542

Piper AM (1944) A graphical interpretation of water-analysis. Trans Am Geophys Union 25:914–928

Ramesh RP, Fan Z, Faizan UR, Guanxing W, Ming Y, Chen Z, Handuo T (2018) Spatiotemporal variations of hydrogeochemistry and its controlling factors in the Gandaki River Basin. Cent Himalaya Nepal Sci Total Environ 622(623):770–782

Rencher AC (2002) Methods of multivariate analysis, 2nd edn. Wiley, New Jersey p, p 732

Saha S, Selim Reza AHM, Roy MK (2019) Hydrochemical evaluation of groundwater quality of the Tista floodplain, Rangpur, Bangladesh. Appl Water Sci 9:198

Saleem A, Dandigi MN, Kumar KV (2012) Correlation-regression model for physico-chemical quality of groundwater in the South Indian city of Gulbarga. Afr J Environ Sci Technol 6(9):353–364

Sara V, Charlotte W, Djoret D, Aminu MB (2016) Interaction entre les eaux souterraines et les eaux de surface dans les plaines inondables du Bas-Logone. Projet gestion durable des eaux du Lac-Tchad. Rapport technique n°10. Hanovre. p 55

Sawyer GN, McCartly DL (1967) Chemistry of sanitary engineers, 2nd edn. McGraw-Hill, New York, p 518

Van Schmus WR, Oliveira EP, Da Silva Filho AF, Toteu SF, Penaye J, Guimarães IP (2008) Proterozoic links between the Borborema Province, NE Brazil, and the Central African Fold Belt. In: Pankhurst RJ, Trouw RAJ, de Brito Neves BB, De Wit MJ (eds), West Gondwana. Pre-Cenozoic correlations acrossthe South Atlantic Region, 294. Geological Society, London. Special Publication, pp 69–99

Schoeller H (1967) Qualitative evaluation of ground water resources (in methods and techniques of groundwater investigations and development), water resources series. UNESCO 33:44–52

Selvam S, IruthayaJeba Dhana Mala R, Muthukakshmi V (2013) A hydrochemical analysis and evaluation of groundwater quality index in Thoothukudi district, Tamilnadu, South India. Int J Adv Eng Appl 2(3):25–37

Shawgar K, Mohammad J, Homayoon K, Ahmadn FM (2020) Groundwater hydrogeochemical assessment using advanced spatial statistics methods: a case study of Tehran-Karaj plain aquifer. Iran Arab J Geosci 13:84

Siva BS, Kamble RB (2017) Precipitation controlled spatial variations in groundwater quality indices-suitability for drinking and irrigation purposes in the basalts of South India. Arab J Geosci 10(171):1–20

Somasundaram MV, Ravindran G, Tellam JH (1993) Groundwater pollution of the Madras urban aquifer, India. Groundwater 31:4–11

Srinivasamoorthy K, Chidambaram S, Prasanna MV, Vasanthavihar M, Peter J, Anandhan P (2008) Identification of major sources controlling groundwater chemistry from a hard rock terrain—a case study from Mettur taluk, Salem district, Tamil Nadu. J Earth Syst Sci 117:49–58

Srinivasamoorthy K, Vasanthavigar M, Vijayaraghavan K, Sarathidasan R, Gopinath S (2013) Hydrochemistry of groundwater in a coastal region of Cuddalore district, Tamilnadu, India: implication for quality assessment. Arab J Geosci 6:441–454

Srinivasamoorthy K, Gopinath M, Chidambaram S, Vasanthavigar M, Sarma VS (2014) Hydrochemical characterization and quality appraisal of groundwater from Pungar sub basin, Tamilnadu, India. J King Saud Univ-Sci 26:37–52

Stoops G (2003) Guidelines for analysis and description of soil and regolith thin sections. Soil Society of America Inc, Madison, Wisconsin

Subba Rao N, Saroja Nirmal I, Suryanarayana K (2005) Groundwater quality in a coastal area-a case study from Andhra Pradesh. India Environ Geol 48:534–550

Subba Rao N, Subrahmanyam A, Ravi Kumar S, Srinivasulu N, Babu Rao G, Surya Rao P, Venktram Reddy G (2012a) Geochemistry and quality of groundwater of Gummanampadu Sub-basin, Guntur district, Andhra Pradesh. India Environ Earth Sci 67:1451–1471

Subba Rao N, Surya Rao P, Venktram Reddy G, Nagamani M, Vidyasagar G, Satyanarayana NLVV (2012b) Chemical characteristics of groundwater and assessment of groundwater quality in Varaha River Basin, Visakhapatnam District, Andhra Pradesh. India Environ Monit Assess 184:5189–5214

Subba Rao N, Marghade D, Dinakar A, Chandana I, Sunitha B, Ravindra B, Balaji T (2017) Geochemical characteristics and controlling factors of chemical composition of groundwater in a part of Guntur district, Andhra Pradesh. India Environ Earth Sci 76:747

Takem GE, Kuitcha D, Ako AA, Mafany GT, Takounjou-Fouepe A, Ndjama J, Ntchancho R, Ateba BH, Chandrasekharam D, Ayonghe SN (2015) Acidification of shallow groundwater in the unconfined sandy aquifer of the city of Douala, Cameroon, Western Africa: implications for groundwater quality and use. Environ Earth Sci 61:287–298

Tamma Rao G, Gurunadha Rao VVS, Srinivasa Rao Y, Ramesh G (2013) Study of hydrogeochemical processes of the groundwater in Ghatprabha river sub-basin, Bagalkot District, Karnataka. India. Arab J Geosci 6(7):2447–2459. https://doi.org/10.1007/s12517-012-0535-4

Tanyileke G (1994) Fluid geochemistry of CO2-rich lakes and soda springs along the Cameroon volcanic line, Cameroon. Ph.D Thesis, Graduate School of Natural Science and Technology, Okayama University, Japan

Todd DK (1980) Groundwater hydrology. Wiley, New York

Toteu SF (1990) Geochemical characterization of the main petrographical and structural units of northern Cameroon: implications for Pan-African evolution. J Afr Earth Sci 10:615–624

Toteu SF, Michard A, Bertrand JM, Rocci G (1987) U-Pb dating of Precambrianrocks from northern Cameroon, orogenic evolution and chronology of the Pan-African belt of central Africa. Precambrian Res 37:71–87

Toteu SF, Van Schmus WR, Penaye J, Michard A (2001) New U-Pb and Sm–Nddata from north-central Cameroon and its bearing on pre-Pan-African history of central Africa. Precambrian Res 108:45–73

Toteu SF, Penaye J, Poudjom Djomani Y (2004) Geodynamic evolution of the Pan-African belt of Central Africa with special reference to Cameroon. Can J Earth Sci 41:73–85

Toteu SF, Penaye J, Deloule E, Van Schmus WR, Tchameni R (2006) Diachronous evolution of volcano-sedimentary basins North of the Congo cra-ton: insights from U-Pb ion microprobe dating of zircons from the Poli, Lom and Yaounde Series (Cameroon). J Afr Earth Sci 44:428–442

Tsozué D, Ndjigui P-D (2017) Geochemical features of the weathered materials developed on gabbro in a semi-arid zone. North Cameroon Geosc 7:16

Van der Merwe JH (1962) Strains in crystalline overgrowths. Philos. Mag. (1798–1977) 7(80):1433–1434

Wakida FT, Lerner DN (2005) Non-agricultural sources of groundwater nitrate: a review and case study. Water Res 39:3–16

WHO (2004) Water for health: guidelines for drinking-water quality, 4th edn. World Health Organization, Geneva, p 541

Wirmvem MJ, Ohba T, Fantong WY, Ayonghe SN, Suila JY, Asaah ANE, Tanyileke G, Hell JV (2013) Hydrogeochemistry of shallow groundwater and surface water in the Ndop plain, NorthWest Cameroon. Afr J Environ Sci Technol 7(6):518–530

Xiao J, Jin ZD, Wang J, Zhang F (2015) Hydrochemical characteristics, controlling factors and solute sources of groundwater within the Tarim River Basin in the extreme arid region. NW Tibet Plateau Quat Int 380(381):237–246

Zghibi A, Merzougui A, Zouhri L, Tarhouni J (2014) Understanding groundwater chemistry using multivariate statistics techniques to the study of contamination in the Korba unconfined aquifer system of Cap-Bon (North-east of Tunisia). J Afr Earth Sci 89:1–15

Zuddas P (2010) Water-Rock interaction processes seen through thermodynamics. Elements 6(5):305–308